AFFDL-TR-77-10

AD A042024

PREDICTION TECHNIQUES FOR THE CHARACTERISTICS OF FIN GENERATED THREE DIMENSIONAL SHOCK WAVE TURBULENT BOUNDARY LAYER INTERACTIONS

HIGH SPEED AERO PERFORMANCE BRANCH (FXG)
AEROMECHANICS DIVISION (FX)

MAY 1977

TECHNICAL REPORT AFFDL–TR–77–10

FINAL REPORT FOR PERIOD JANUARY 1974 - SEPTEMBER 1976

Approved for public release; distribution unlimited

D D C
RECEIVED
JUL 27 1977
D

AIR FORCE FLIGHT DYNAMICS LABORATORY
AIR FORCE WRIGHT AERONAUTICAL LABORATORIES
AIR FORCE SYSTEMS COMMAND
WRIGHT–PATTERSON AIR FORCE BASE, OHIO 45433

AD NO.
DDC FILE COPY

NOTICE

When Government drawings, specifications, or other data are used for any purpose other than in connection with a definitely related Government procurement operation, the United States Government thereby incurs no responsibility nor any obligation whatsoever; and the fact that the government may have formulated, furnished, or in any way supplied the said drawings, specifications, or other data, is not to be regarded by implication or otherwise as in any manner licensing the holder or any other person or corporation, or conveying any rights or permission to manufacture, use, or sell any patented invention that may in any way be related thereto.

This report has been reviewed by the Office of Information (OI) and is releasable to the National Technical Information Service (NTIS). At NTIS, it will be available to the general public, including foreign nations.

This technical report has been reviewed and is approved for publication.

James R. Hayes
Project Engineer

FOR THE COMMANDER

Alfred C. Draper
ALFRED C. DRAPER
Asst. For Research and Technology
Flight Mechanics Division

Copies of this report should not be returned unless return is required by security considerations, contractual obligations, or notice on a specific document.

AIR FORCE - 14 JUL 77 - 125

UNCLASSIFIED

SECURITY CLASSIFICATION OF THIS PAGE (When Data Entered)

REPORT DOCUMENTATION PAGE

READ INSTRUCTIONS BEFORE COMPLETING FORM

1. REPORT NUMBER: AFFDL-TR-77-10

2. GOVT ACCESSION NO.

3. RECIPIENT'S CATALOG NUMBER

4. TITLE (and Subtitle): PREDICTION TECHNIQUES FOR THE CHARACTERISTICS OF FIN GENERATED THREE DIMENSIONAL SHOCK WAVE TURBULENT BOUNDARY LAYER INTERACTIONS.

5. TYPE OF REPORT & PERIOD COVERED: Final Report, January 1974 to Sept 1976

6. PERFORMING ORG. REPORT NUMBER

7. AUTHOR(s): James R. Hayes

8. CONTRACT OR GRANT NUMBER(s)

9. PERFORMING ORGANIZATION NAME AND ADDRESS:
Air Force Flight Dynamics Laboratory
High Speed Aero Performance Branch (FXG)
Wright-Patterson Air Force Base, Ohio 45433

10. PROGRAM ELEMENT, PROJECT, TASK AREA & WORK UNIT NUMBERS:
Project No. 1366
Task No. 136603
Work Unit No. 13660329

11. CONTROLLING OFFICE NAME AND ADDRESS:
Air Force Flight Dynamics Laboratory
Aeromechanics Division (FX)
Wright-Patterson Air Force Base, Ohio 45433

12. REPORT DATE: May 1977

13. NUMBER OF PAGES: 67

14. MONITORING AGENCY NAME & ADDRESS (if different from Controlling Office)

15. SECURITY CLASS. (of this report): Unclassified

15a. DECLASSIFICATION DOWNGRADING SCHEDULE

16. DISTRIBUTION STATEMENT (of this Report)

Approved for public release, distribution unlimited.

17. DISTRIBUTION STATEMENT (of the abstract entered in Block 20, if different from Report)

18. SUPPLEMENTARY NOTES

19. KEY WORDS (Continue on reverse side if necessary and identify by block number)
Three-dimensional Interaction
Turbulent Boundary Layer
Boundary Layer Separation
Peak Heating
Peak Pressure

20. ABSTRACT (Continue on reverse side if necessary and identify by block number)

The characteristics of the three-dimensional shock wave turbulent boundary layer interaction were investigated through an extensive experimental test program. This program encompassed Mach numbers from 2.95 to 5.85, Reynolds numbers of 1.5 x 10^6 per foot, and boundary layer thicknesses at the fin leading edge from 0.13 to 6 inches. Each test collected heat transfer, pressure, and oil flow data at selected fin deflection angles ranging from 0° to 20°. The objective was to generate a data base convering a wide enough range of

DD FORM 1 JAN 73 1473 EDITION OF 1 NOV 65 IS OBSOLETE

UNCLASSIFIED

SECURITY CLASSIFICATION OF THIS PAGE (When Data Entered)

012070 1

20. ABSTRACT (Cont'd)

parameters to allow the formulation of a set of inclusive prediction techniques for the major characteristics of the interaction.

This report presents the results of the experimental program and the correlations developed from the data. It was found that most of the interaction characteristics were dependent on the value of the shock strength (M_∞ Sin θ) and on the distance aft of the fin leading edge measured in boundary layer thicknesses (X/δ).

Correlations are developed for the peak pressure and heat transfer rate and their location. The separation pressure ratio and the plateau pressure ratio are correlated with 2-D data substantiating Spaid's conclusion that the separation phenomena is independent of the method used to generate it. The location of the separation line is also determined and correlation on the pressure distribution through the interaction are presented.

FOREWORD

This document presents the results of an experimental and analytical investigation into the characteristics of the three dimensional shock wave turbulent boundary layer interaction. The study was conducted by the High Speed Aero Performance Branch (FXG), Aeromechanics Division, Air Force Flight Dynamics Laboratory, Wright Patterson Air Force Base, Ohio. The work concludes an in-house and contracted research program and was performed under Project 1366 "Aeroperformance and Aeroheating Technology", Task 136603 "Aerodynamic Heating to Military Vehicles". This report covers experimental work conducted from January 1974 to September 1976 and concludes work unit 13660329 "Design Techniques to Predict and Minimize Interference Heating'.

The contracted research effort was as follows. Contract F33615-73-C-3133 was with Princeton University, Department of Aerospace and Mechanical Sciences, Princeton, New Jersey and covered the period of April 1973 through November 1974. This contractor investigated and reported on heat transfer, surface pressure, and flow field data for Mach 2.95. Contract F33615-73-C-3046 with McDonnell Douglas Corporation, St. Louis, Missouri covered the period of January 1973 through April 1974. This contractor investigated and reported on pressure data and Heat Transfer at Mach 3.71.

ACCESSION for
NTIS White Section ☑
DDC Buff Section ☐
UNANNOUNCED ☐
JUSTIFICATION
BY
DISTRIBUTION/AVAILABILITY CODES
Dist AVAIL and/or SPECIAL
A

Preceding Page Blank - NOT FILMED

TABLE OF CONTENTS

SECTION		PAGE
I	INTRODUCTION	1
	1. Basic 3-D Interaction Characteristics	3
II	PRESSURE PROFILES	6
	1. Peak Pressure Ratio	6
	2. Pressure Ratio Under the Shock	8
	3. Plateau Pressure Ratio	12
	4. Separation Pressure Ratio	14
	5. Onset of Pressure Rise	19
	6. Pressure Distributions	22
	a. Inner Region	22
	b. Outer Region	29
III	HEAT TRANSFER PROFILES	34
	1. Peak Heat Transfer	34
	2. Heat Transfer Distributions	47
IV	CONCLUSIONS	53
REFERENCES		54

LIST OF ILLUSTRATIONS

FIGURE		PAGE
1	Basic Interaction Characteristics	4
2	Peak Pressure Correlation Method	7
3	Exponent in Peak Pressure Correlation	9
4	Peak Pressure and Heating Location	10
5	Pressure Trough Development	11
6	Shock Pressure Correlation	13
7	Plateau Pressure Correlation	15
8	Separation Pressure Correlation	16
9	Separation Location Coordinate System	17
10	Slope of Separation Asymptote	18
11	Separation Asymptote Parameter "a"	20
12	Separation Coordinates as a Function of M_∞ Sin Θ	21
13	Onset Pressure Gradient at Mach 2.95	23
14	Onset Pressure Gradient at Mach 3.71	24
15	Onset Pressure Gradient at Mach 3.75	25
16	Onset Pressure Gradient at Mach 4.51	26
17	Onset Pressure Gradient at Mach 5.04	27
18	Onset Pressure Gradient Correlation	28
19	Pressure Distribution, Peak-to-Shock	30
20	Pressure Distribution, Plateau-to-Separation	31
21	Pressure Distribution, Separation-to-Onset	32
22	Peak Heating at Mach 2.95	35
23	Peak Heating at Mach 3.00	36
24	Peak Heating at Mach 3.01	37
25	Peak Heating at Mach 3.71	38
26	Peak Heating at Mach 3.75	39
27	Peak Heating at Mach 4.51	40
28	Peak Heating at Mach 4.75	41
29	Peak Heating at Mach 5.04	42
30	Coefficient in Peak Heating Correlation	43
31	Amplification of Peak Heating Due to Vorticity	45

LIST OF ILLUSTRATIONS (Cont'd)

FIGURE		PAGE
32	Comparison of Peak Pressure and Heating Location	46
33	Pressure Gradient Parameter	48
34	Effect of Pressure Gradient Parameter	50
35	Effect of Velocity Gradient Parameter	51
36	Heating Rate Under the Shock	52

LIST OF TABLES

TABLE		PAGE
1	Data Base	2

LIST OF SYMBOLS

Symbol		Units
a	Separation Asymptote Parameter (Figure 10)	in.
b	Separation Asymptote Parameter (Figure 10)	in.
b/a	Slope of Separation Asymptotes (Figure 11)	
C	Pressure Gradient Parameter (Equation 11)	
h	Heat Transfer Coefficient	$\frac{Btu}{ft^2\text{-sec -}^\circ R}$
M	Mach Number	
n	Velocity Gradient Parameter (Equation 12)	
n_p	Exponent in Peak Pressure Correlation (Equation 1)	
n_{St}	Coefficient in Peak Heating Correlation (Equation 7)	
P	Pressure	psia
St	Stanton Number	
X	Distance from Fin Leading Edge in the Freestream Direction	in.
$\overline{X}$	Separation Coordinate Axis (Figure 10)	in.
Y	Distance from Fin Leading Edge Normal to Freestream Direction	in.
$\overline{Y}$	Separation Coordinate Axis (Figure 10)	in.
Z	Distance Normal to Flat Plate Surface	in.
α	Fin Deflection Angle	deg.
δ	Boundary Layer Thickness	in.
Θ	Shock Wave Angle	deg.
ϕ	Angle to Peak Pressure and Heating Location	deg.
ψ	Distance from Shock Toward Fin in Direction Normal to Fin (Equation 10)	in.

Subscripts

FP	Flat Plate or Undisturbed Value
inc.	Incipient Separation Condition
ON	Onset Condition
PK	Peak Value
PL	Plateau Value

LIST OF SYMBOLS (Cont'd)

Subscripts

SEP	Separation Value
SH	Shock Value
VD	Van Driest Calculation
∞	Condition Outside Interaction Region
1	Condition Upstream of Oblique Shock
2	Condition Downstream of Oblique Shock

SUMMARY

The characteristics of the three dimensional shock wave turbulent boundary layer interaction were investigated through an extensive experimental test program. This program encompassed Mach numbers from 2.95 to 5.85, Reynolds numbers of 1.5×10^6 to 28×10^6 per foot, and boundary layer thicknesses at the fin leading edge from 0.13 to 6 inches. Each test collected heat transfer, pressure, and oil flow data at selected fin deflection angles ranging from 0° to 20°. The objective was to generate a data base covering a wide enough range of parameters to allow the formulation of a set of inclusive empirical prediction techniques for the major characteristics of the interaction.

This report presents the results of the experimental program and the correlations developed from the data. It was found that most of the interaction characteristics were dependent on the value of the shock strength ($M_\infty \sin\theta$) and on the distance aft of the fin leading edge measured in boundary layer thicknesses (X/δ). The correlations developed for the peak pressure and peak heating were

$$\frac{P_{PK}}{P_{FP}} = (M_\infty \sin\theta)^{n_p} \quad \text{and} \quad \frac{St_{PK}}{St_{FP}} = n_{St}\,(M_\infty \sin\theta - 1) + 0.75$$

where n_p and n_{St} are functions of X/δ. At large X/δ it was observed that $n_p \simeq 2.40$ and $n_{St} \simeq 4.75$. Both represent values substantially higher than 2-D peak values. By correlating 2-D and 3-D plateau pressures in the separated region Spaid's conclusion that the separation phenomena is independent of the method used to generate it was substantiated and extended to 3-D interactions. The extent of the interaction region was determined by correlating the location of the separation line. It was observed that the separation line could be described by a set of hyperbolic curves when the correct coordinate system was established. These hyperbolic curves were defined by correlating the slope and intercepts of their asymptotes as a function of $M_\infty \sin\theta$.

Complementing the above results are correlations on the shock and separation pressure ratios, the location of the peak pressure and heat transfer rate, and the pressure distribution through the interaction region.

Preceding Page Blank - Filmed

SECTION I

INTRODUCTION

Sustained flight at high Mach numbers presents a variety of problems to the engineer. A fundamental and highly influencial phenomenon is that of the shock wave boundary layer interaction. This flow field interaction is characterized by boundary layer separation and by localized areas of high pressure and high aerodynamic heating which impact on the design of empennages and control surfaces.

The two dimensional interaction has received much experimental attention and commonly occurs on flight vehicles at control surface hinge lines. The three dimensional interaction, characteristically generated by deflected fins and boundary layer diverters, has received less attention although it produces more severe pressure and heating problems. Moreover, the published data on 3-D interactions generally presents conflicting trends in peak pressure and peak heating correlations. This undoubtedly is a result of the complexity of the interaction and the fact that no single investigator has obtained data over a sufficient range of Mach numbers, Reynolds numbers, and fin deflection angles.

The Air Force Flight Dynamics Laboratory (AFFDL) has an ongoing program involved in the collection and generation of 3-D interaction data. The objective is to obtain data over a wide enough range of the above parameters to allow the formulation of an inclusive prediction technique for the major interaction characteristics. This report presents the current results of the program.

Table 1 presents the data base on which the correlations in this report were made. Oskam, Bogdonoff, and Vas (Reference 1) carried out a study at Mach 2.95 in the Princeton University high Reynolds number tunnel. In this investigation two model configurations were employed to study the effect of boundary layer thickness on the interaction. A boundary layer thickness of 0.13 inch at the fin leading edge was obtained by mounting a fin on a sharp flat plate suspended between the tunnel side

TABLE 1

DATA BASE

M_∞	Re/ft † $\times 10^{-6}$	δ	FIN DEFLECTION ANGLES ~ DEG. PRESSURE 0	2	4	6	8	10	12	14	16	18	20	HEAT TRANSFER 0	2	4	6	8	10	12	14	16	18	20	OIL FLOW 0	2	4	6	8	10	12	14	16	18	20
2.95	19.2	0.18†		■	■	■	■	■	■	■																■	■	■	■	■	■	■			
2.95	19.2	0.55†		■	■	■	■	■	■	■					■	■	■	■	■	■	■					■	■	■	■	■	■	■			
3.00	3.24	0.135†	■		■		■	■						■		■		■	■								■	■	■	■					
3.71	1.50	6.0†		■	■	■	■	■	■	■	■	■	■		■	■	■	■	■	■	■	■	■	■											
3.71	3.50	6.0†		■	■	■	■	■	■	■	■	■	■		■	■	■	■	■	■	■	■	■	■			■		■		■		■		■
3.75	3.28	0.162†	■		■		■		■		■		■	■		■		■		■		■		■		■	■	■	■						
4.50	3.23	0.150†	■		■		■		■		■		■	■		■		■		■		■		■			■		■		■		■		■
4.75	7.76	0.26‡	■								■		■	■	■	■	■	■	■	■	■	■	■	■										■	■
5.04	7.38	0.26‡	■						■	■	■	■	■	■	■	■	■	■	■	■	■	■	■	■	■	■	■	■	■	■	■	■	■	■	■
5.85	11.0	0.246†				■	■	■	■		■		■			■	■	■	■	■		■		■											
5.85	28.0	0.21†				■	■	■	■		■		■			■	■	■	■	■		■		■			■	■	■	■	■		■		■

† Evaluated by pitot pressure survey

‡ Scaled from shadowgraphs

walls. The second configuration mounted the fin directly on the floor of the tunnel to obtain a boundary layer thickness of 0.55 inch at the fin leading edge. A similar study was made in the NASA Langley Unitary Plan Tunnel. Token (Reference 2) carried out a study at Mach 3.71 in which a fin 15 inches high and 32 inches long was mounted on the tunnel side wall in a 6 inch boundary layer. In a follow up study (Reference 3) AFFDL mounted the same fin on a sharp flat plate 6 feet long, and suspended the plate from the tunnel side wall. Data were obtained at Mach numbers of 3.0 and 3.7 with boundary layer thicknesses ranging from 0.37 to 0.43 inches.

A large amount of data have been obtained in the AEDC-VKF Tunnels A and B. A small flat plate model 18 inches long and 10 inches wide was employed in Tunnel A. A fin 7.5 inches long and 3 inches high was mounted on the plate. AFFDL obtained data (Reference 4) at Mach numbers of 3.0, 3.75, and 4.5 with this configuration. The same fin was then mounted on a plate 24 inches square and installed in Tunnel B. The author obtained data on this model at Mach 4.75 and 5.04. This previously unpublished data was presented at the American Institute of Aeronautics and Astronautics (AIAA) 15th Aerospace Sciences Meeting (Reference 5).

The model employed in the Tunnel A test was also installed in the AFFDL Mach 6 High Reynolds Number Facility. Data (Reference 6) was obtained in this tunnel at a nominal Mach number of 5.85.

The range in Mach number and Reynolds number which the data base covers has made it possible to correlate sets of data which previously were considered to present conflicting data trends.

1. BASIC 3-D INTERACTION CHARACTERISTICS

The typical 3-D interaction generator is shown in Figure 1. It consists of a sharp flat plate instrumented with thermocouples or pressure taps, and a fin mounted normal to the plate which may be set to various deflection angles. Also shown in Figure 1 are typical pressure and heat transfer profiles taken in a plane normal to the undisturbed flow direction.

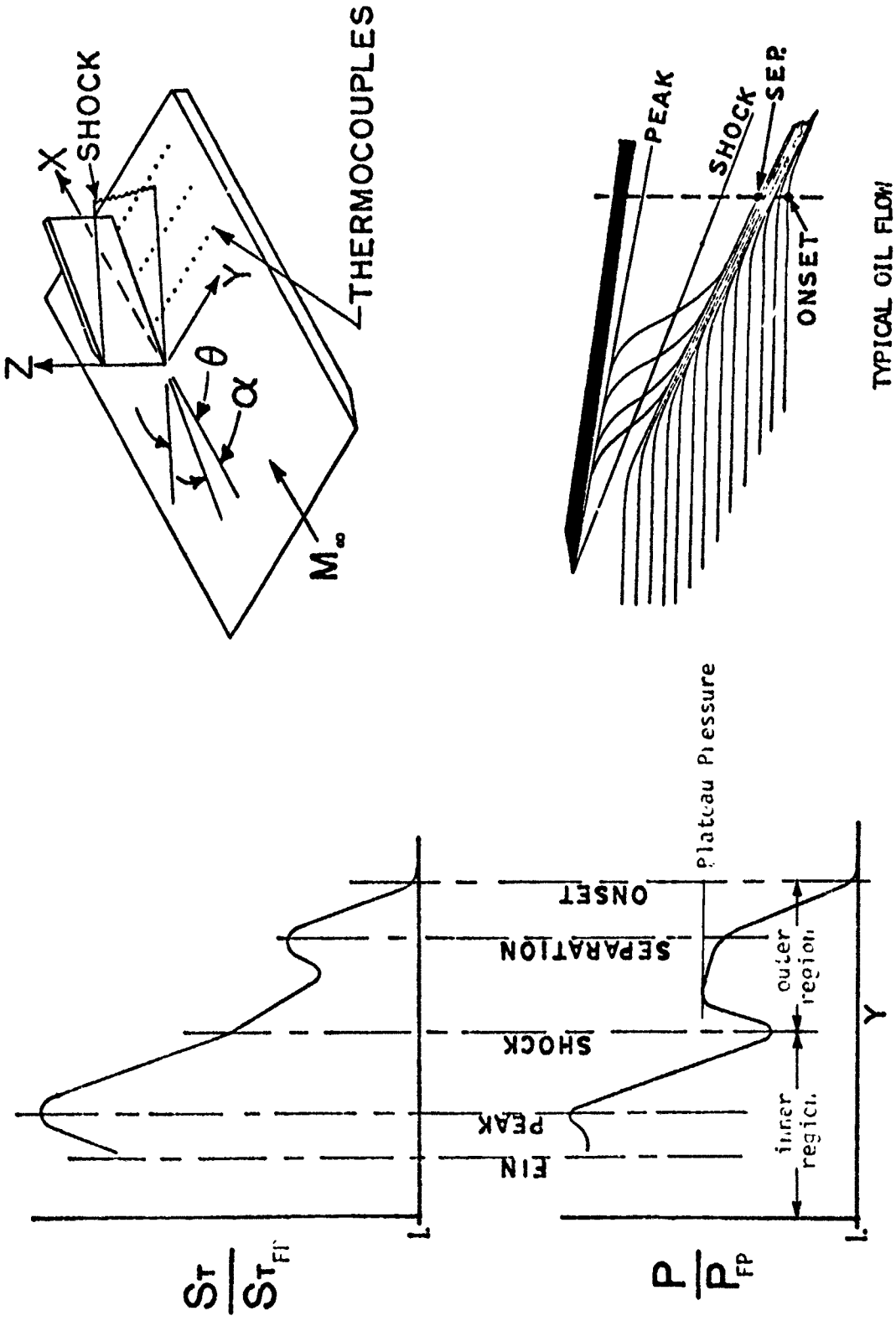

Figure 1. Basic Interaction Characteristics

The pressure distribution may be divided into two distinct regions by the fin oblique shock wave. The outer region extends from onset of the interaction region to the shock wave and is, at sufficient shock strength, a region of separated flow. The flow in this region has distinct two dimensional characteristics. As will be shown later the separation and plateau pressure ratios may be predicted with 2-D data correlations. The inner region, extending from the shock wave to the fin surface, is characterized by the sharp peak in pressure which lies close to the fin. At sufficient shock strength the flow in this region is dominated by an imbedded vortex which produces a trough or low pressure region under the shock wave and peak pressures in excess of oblique shock predictions.

The heat transfer distribution is characterized by a small peak at the line of boundary layer separation, followed by a smooth rise to the shock wave location. At the shock location the slope steepens abruptly as the fin is approached. The large inner peak occurs at approximately the same location as the pressure peak.

When sufficient shock strength is attained to produce separation the oil flow data have characteristics as shown in Figure 1. The peak pressure and heating occur along the line of streamline divergence near the fin. Maximum streamline deflection occurs at the shock location as determined by oblique shock relations. The line of boundary layer separation is observed to be the inner edge of the oil accumulation line and onset is the point at which the undisturbed streamlines first begin to curve.

SECTION II

PRESSURE PROFILES

The features of the pressure profile introduced in Section I-1 which will be discussed are the peak, shock, plateau, and separation pressure magnitudes and their locations in the interaction region. The correlation parameters found to be most successful are the shock strength, M_∞ Sin θ, and the nondimensional distance, "X/δ". The parameter M_∞ Sin θ is the component of the free stream Mach number normal to the fin oblique shock wave, and is calculated from oblique shock relations. This parameter is useful as a measure of the strength of the interaction and as a transformation variable in applying 2-D correlations to the 3-D data. The parameter "X/δ" is the ratio of the distance downstream of the fin leading edge to the boundary layer thickness at the fin leading edge. The interaction region grows in strength and extent with distance aft of the fin leading edge. The pressure in the plateau region remains nearly constant with X/δ, however the peak pressure increases until it is greater than oblique shock predictions.

1. PEAK PRESSURE RATIO

The peak pressure ratios were investigated by plotting on log-log paper the peak pressures as a function of M_∞ Sin θ. At each Mach number and for each X position the result is a straight line passing through $P_{PK}/P_{FP} = 1$ and M_∞ Sin $\theta = 1$. The slope of the line seemed to vary with Mach number and X, however it was found that the apparent Mach number dependence could be removed by considering the dependence on X/δ rather than X. Figure 2 shows several representative plots of the peak pressure data as a function of M_∞ Sin θ and X/δ. They indicate a relationship of the form

$$\frac{P_{PK}}{P_{FP}} = (M_\infty \text{ Sin } \theta)^{n_p} \qquad (1)$$

where n_p is the slope of the curves in Figure 2 and is a function of X/δ.

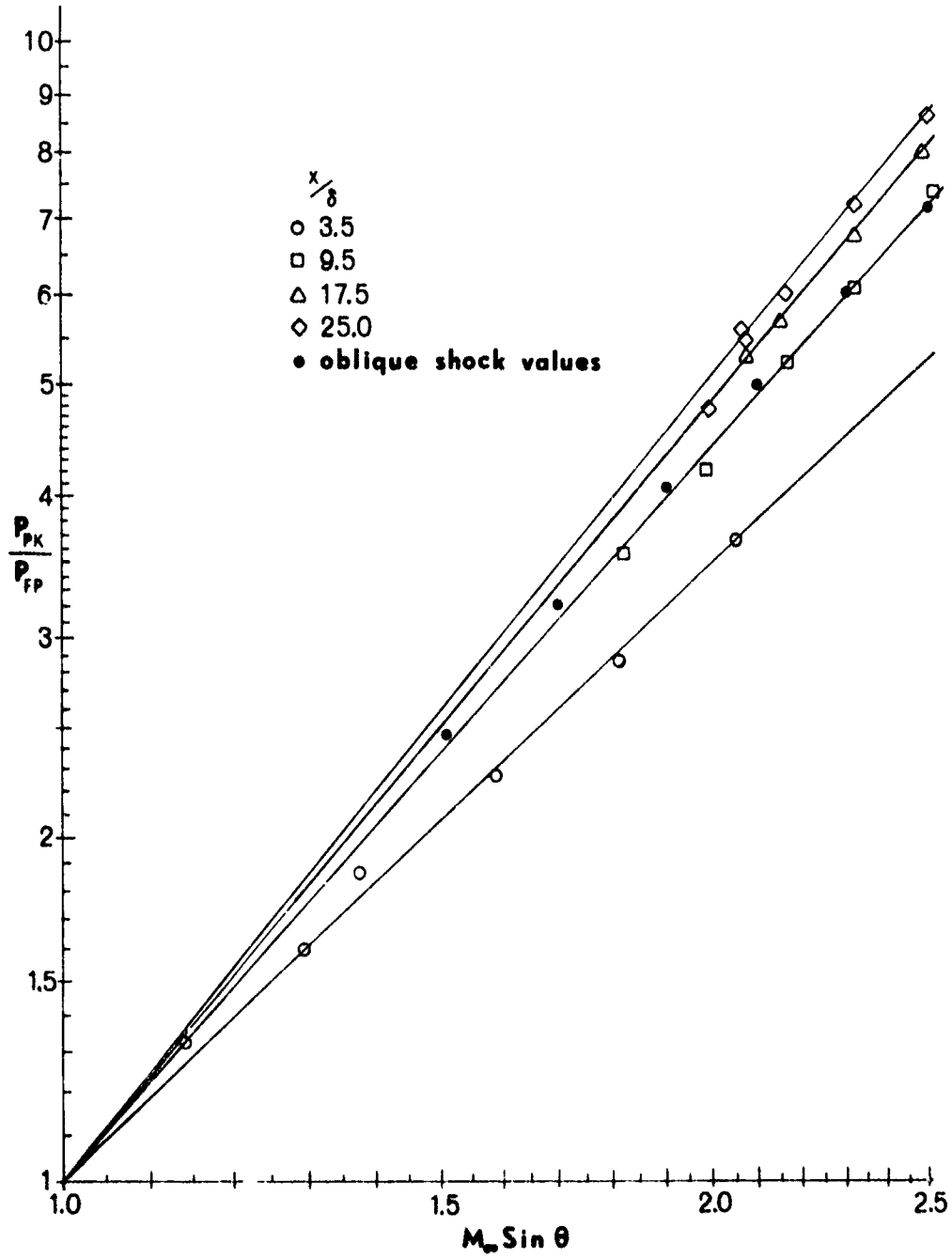

Figure 2. Peak Pressure Correlation Method

All of the available peak pressure data were plotted in the format of Figure 2 and the value of n_p calculated. The function n_p derived is shown in Figure 3. Figure 3 shows that at small X/δ the peak pressure is lower than oblique shock predictions regardless of shock strength. However, the oblique shock values are attained within ten boundary layer thicknesses of the fin apex. At X/δ greater than ten the oblique shock values are exceeded. It should also be noted that the value of n_p approaches a constant value of about 2.4 at large X/δ. This shows that although the pressure continues to increase with shock strength at each X/δ, the rate at which this rise occurs approaches a fixed value. At $X/\delta > 30$ the peak pressure function then is

$$\frac{P_{PK}}{P_{FP}} = (M_\infty \text{ Sin } \theta)^{2.4} \tag{2}$$

for any X/δ.

The peak pressure occurs along a line which may be closely approximated by a ray from the fin leading edge. The angle ϕ between this ray and the free stream direction has been correlated in Figure 4 with the value predicted by Token's expression (Reference 2).

$$\phi = 0.24\ (\theta-\alpha) + \alpha \tag{3}$$

2. PRESSURE RATIO UNDER THE SHOCK

Figure 5 presents the development of the pressure distribution with shock strength. At low shock strength, below that required for incipient separation, the pressure rises smoothly from onset to the peak value. When incipient separation is reached a plateau region begins to form outside the shock wave location. Increased shock strength causes the formation of a trough under the shock wave location. The pressure ratio in this trough varies with shock strength and distance aft of the fin leading edge.

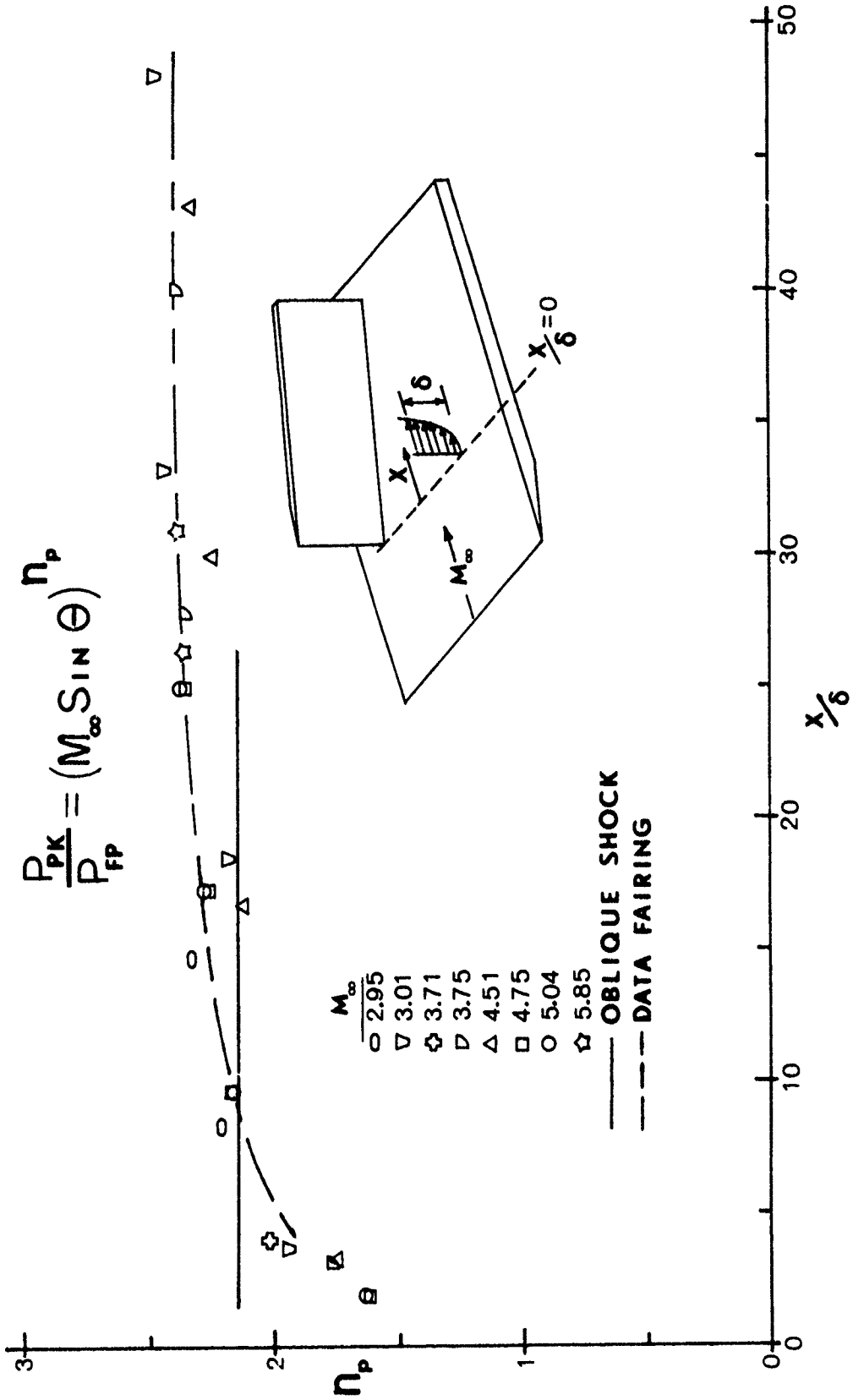

Figure 3. Exponent in Peak Pressure Correlation

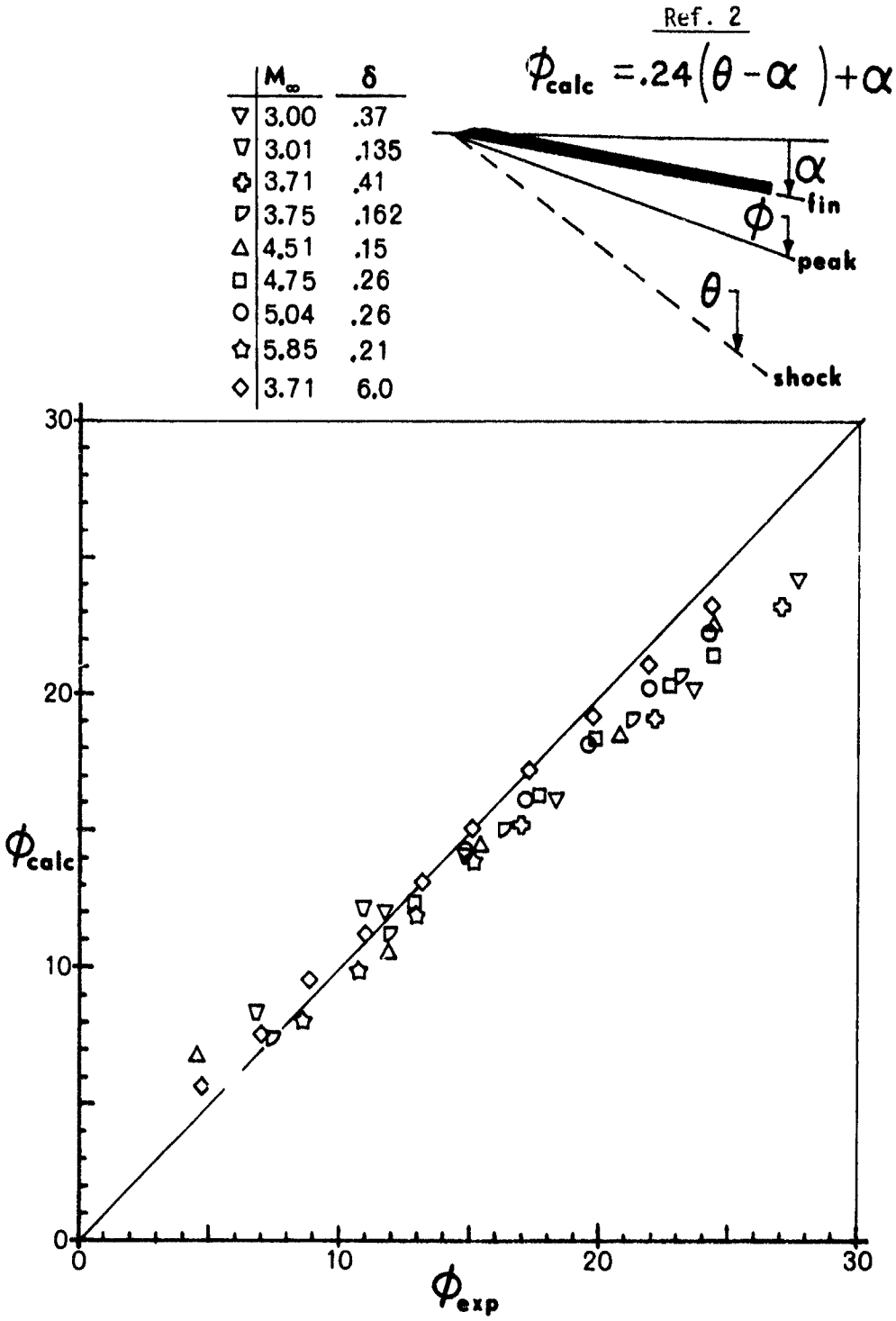

Figure 4. Peak Pressure and Heating Location

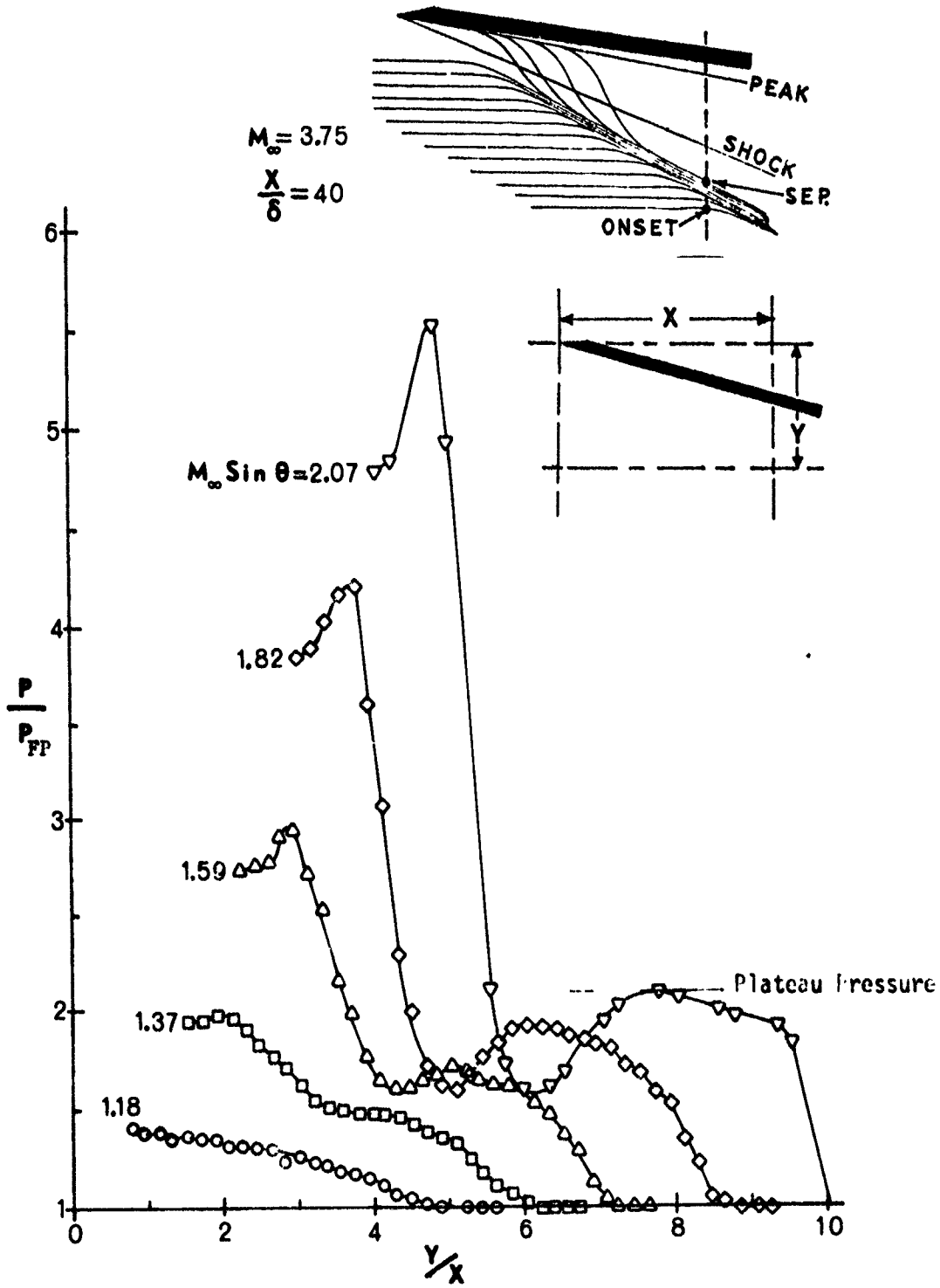

Figure 5. Pressure Trough Development

The first attempt to correlate the shock pressure in the trough was based on the oil flow data which shows that the boundary layer flow inside the shock wave moves outward under the shock and into the separated region. It was thought that the trough pressure level might be determined by the pressure rise across the shock external to the boundary layer. It was also observed that at large X/δ the pressure level in the trough varied with shock strength in a manner similar to that of the unit Reynolds number ratio across the shock. That is, the pressure rises with M_∞ Sin θ to some maximum value and then drops off again as M_∞ Sin θ increases. The maximum pressure occurs at the same shock strength as the maximum Reynolds number ratio. However no conclusive correlation could be found between the shock pressure level and either the Reynolds number or the pressure differential across the shock.

A second and more successful attempt to correlate the trough pressure was based on Token's (Reference 2) work. Token suggested that the peak heating rate could be correlated with stagnation point theory and developed equations for the heating distribution between the peak and shock wave locations. The equations included a pressure gradient term involving the peak and shock pressure ratios. The peak Stanton number was therefore plotted as a function of $(P_{PK} - P_{SH})/P_{FP}$ as shown in Figure 6. The function shows a dependence on X/δ, however the limited amount of data prevents firm conclusions on it's effects from being drawn. Each point on this figure requires accurate heat transfer and pressure data at the peak and shock locations and that the shock strength be large enough to produce the trough. A small percentage of the data base satisfied all these requirements. The data in Figure 6 indicate that this correlation together with the peak pressure and peak heating correlations can be used to determine the shock pressure, however more data is required to increase its utility.

3. PLATEAU PRESSURE RATIO

The flow properties between onset and the shock wave in the 3-D interaction are similar to those in the separated region of a 2-D interaction. If M_∞ Sin θ is used as the Mach number for the interaction then the plateau

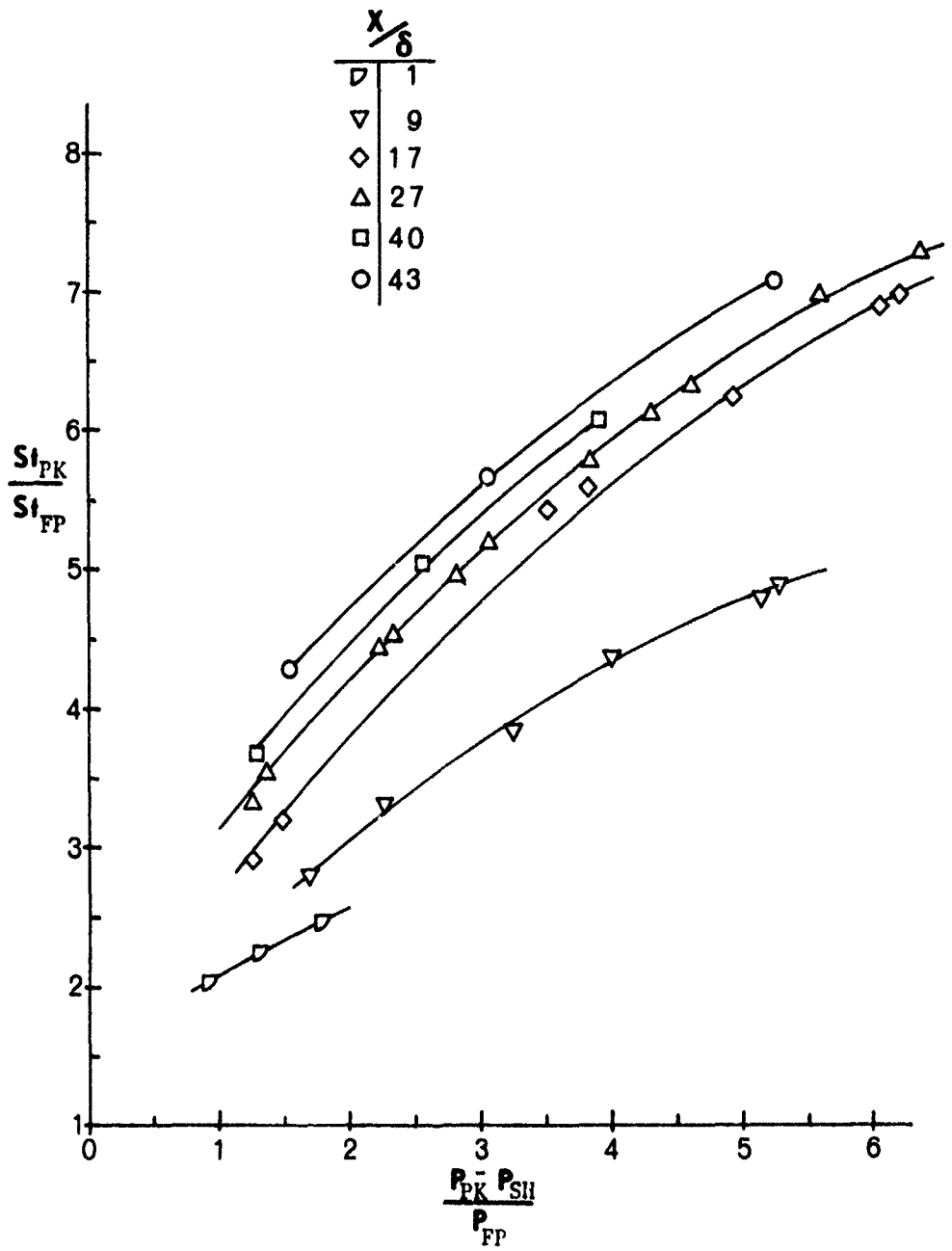

Figure 6. Shock Pressure Correlation

and separation pressures can be predicted by 2-D data correlations. Figure 7 shows the 2-D plateau pressure correlation curves and 2-D and 3-D data superimposed. The plateau pressure is independent of X, δ, and Reynolds number and depends only on the shock strength.

The plateau pressure is a result of the boundary layer separation process and its magnitude is independent of the method used to generate the separation. Data from 2-D shock impingements, ramps, 3-D fin shock impingement, steps, and jet injection all correlate well in the plateau region.

4. SEPARATION PRESSURE RATIO

The boundary layer separation line in the 3-D interaction can be identified in oil flow photographs as the inner edge of the oil accumulation line produced by the convergence of the freestream surface streamlines as shown in Figure 1. The surface pressure at this location agrees well with 2-D separation theory which predicts separation at 73% of the plateau pressure rise. Figure 8 presents the separation pressure data superimposed on a curve representing 73% of the plateau correlation curve.

Accurately locating the separation line without oil flow data is difficult. It was found that the separation pattern around half cones on a flat plate formed hyperbolic curves (Reference 12). This approach was applied to the fin data. A coordinate system was set up with the fin shock wave on the $\overline{X}$ axis and the fin leading edge at a distance "a" from the $\overline{Y}$ axis. In this coordinate system the separation lines form hyperbolic curves. As shown in Figure 9, a hyperbolic curve is defined by its asymptotes. The asymptotes may be described by their slope "b/a" and either "a" or "b"; therefore, the separation line may be defined by two numbers which must be correlated in order to predict separation location. The slope of the asymptotes correlates well with $M_\infty \sin\theta$ as shown in Figure 10. This figure shows that the slope $\frac{b}{a}$ approaches zero at $M_\infty \sin\theta \approx 1.3$. At this shock strength the shock wave and the separation line are coincident. In reality separation no longer exists. The pressure plateau also ceases to exist and the peak pressure approaches the oblique shock value. For shock

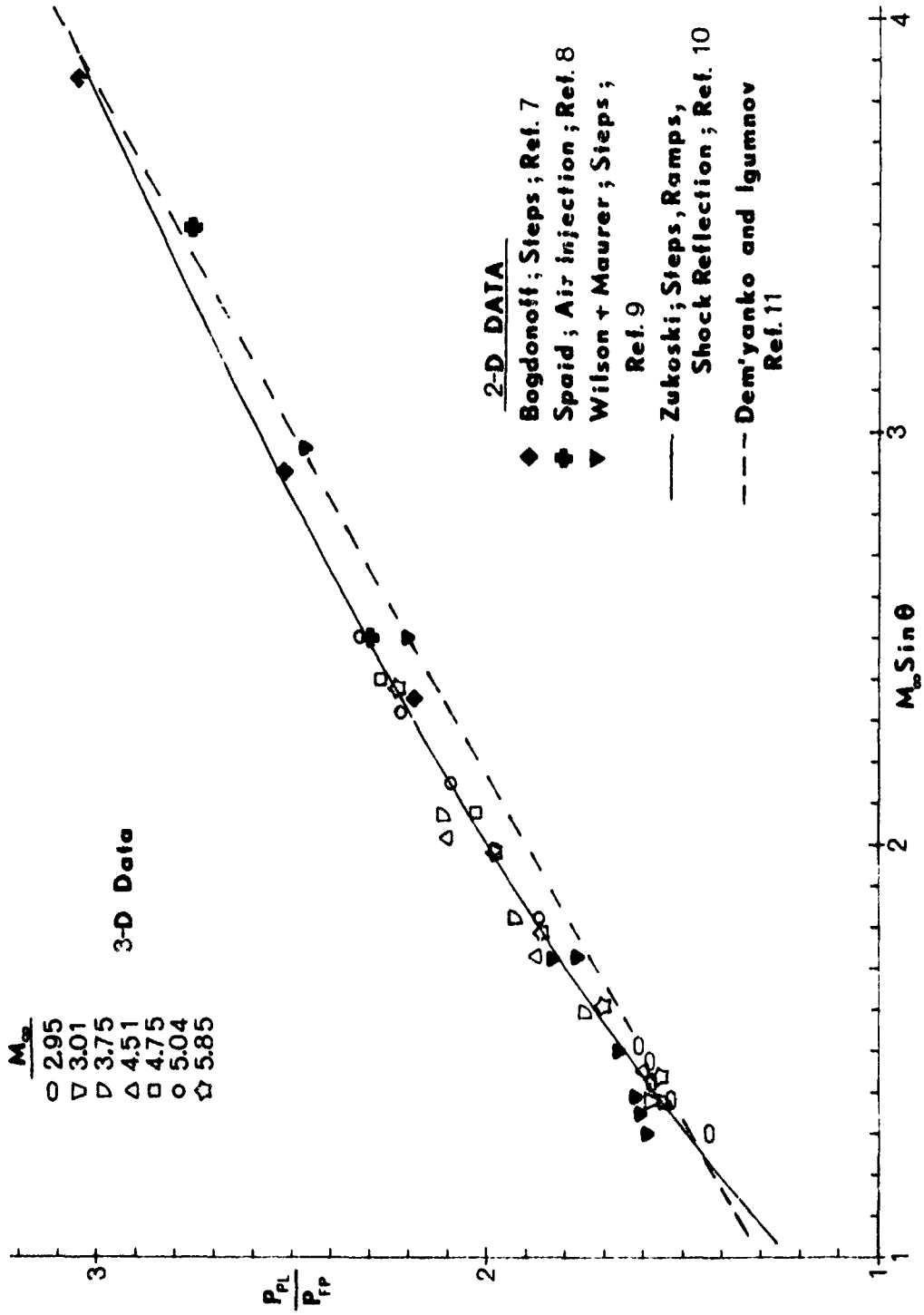

Figure 7. Plateau Pressure Correlation

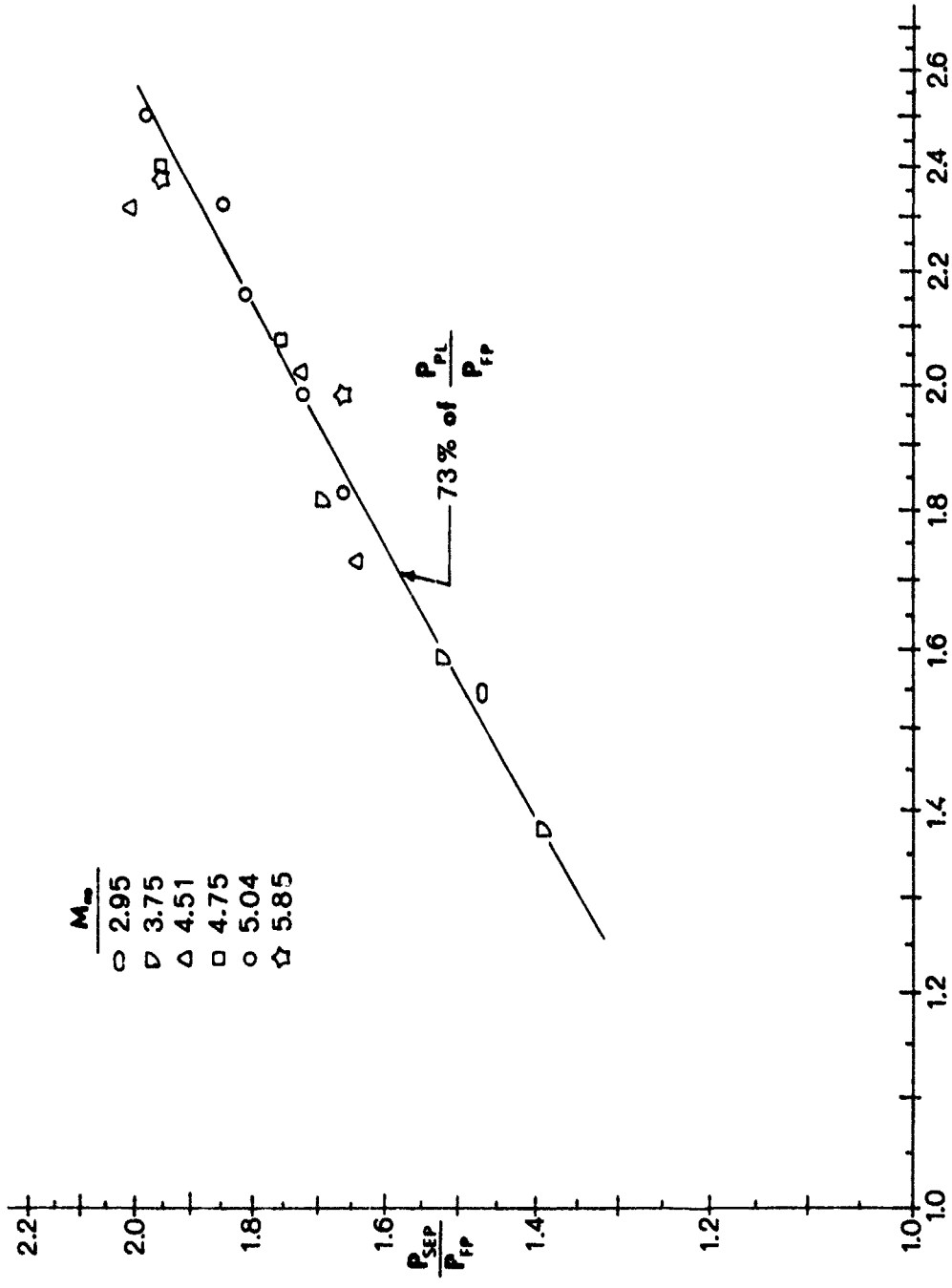

Figure 8. Separation Pressure Correlation

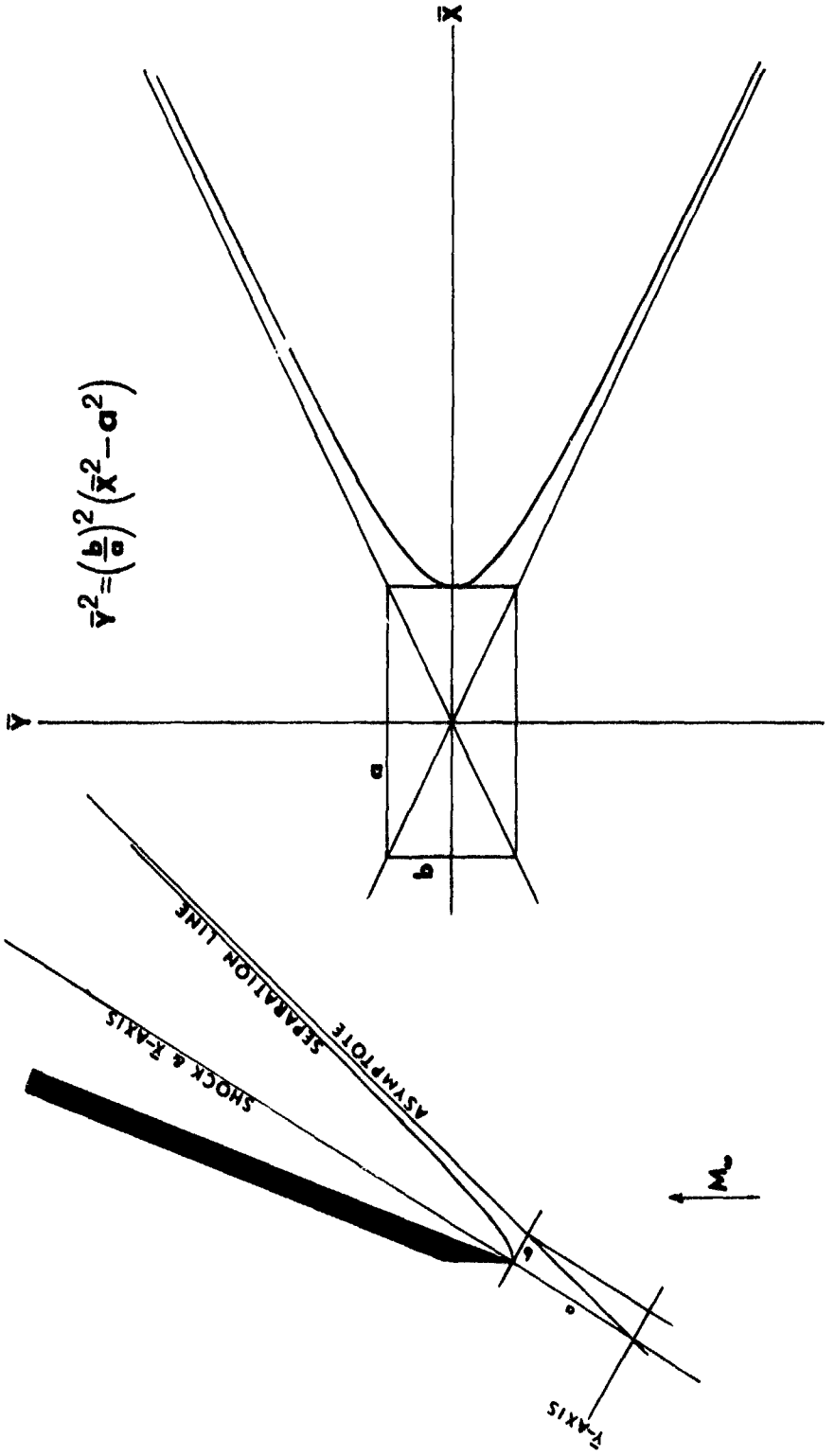

Figure 9. Separation Location Coordinate System

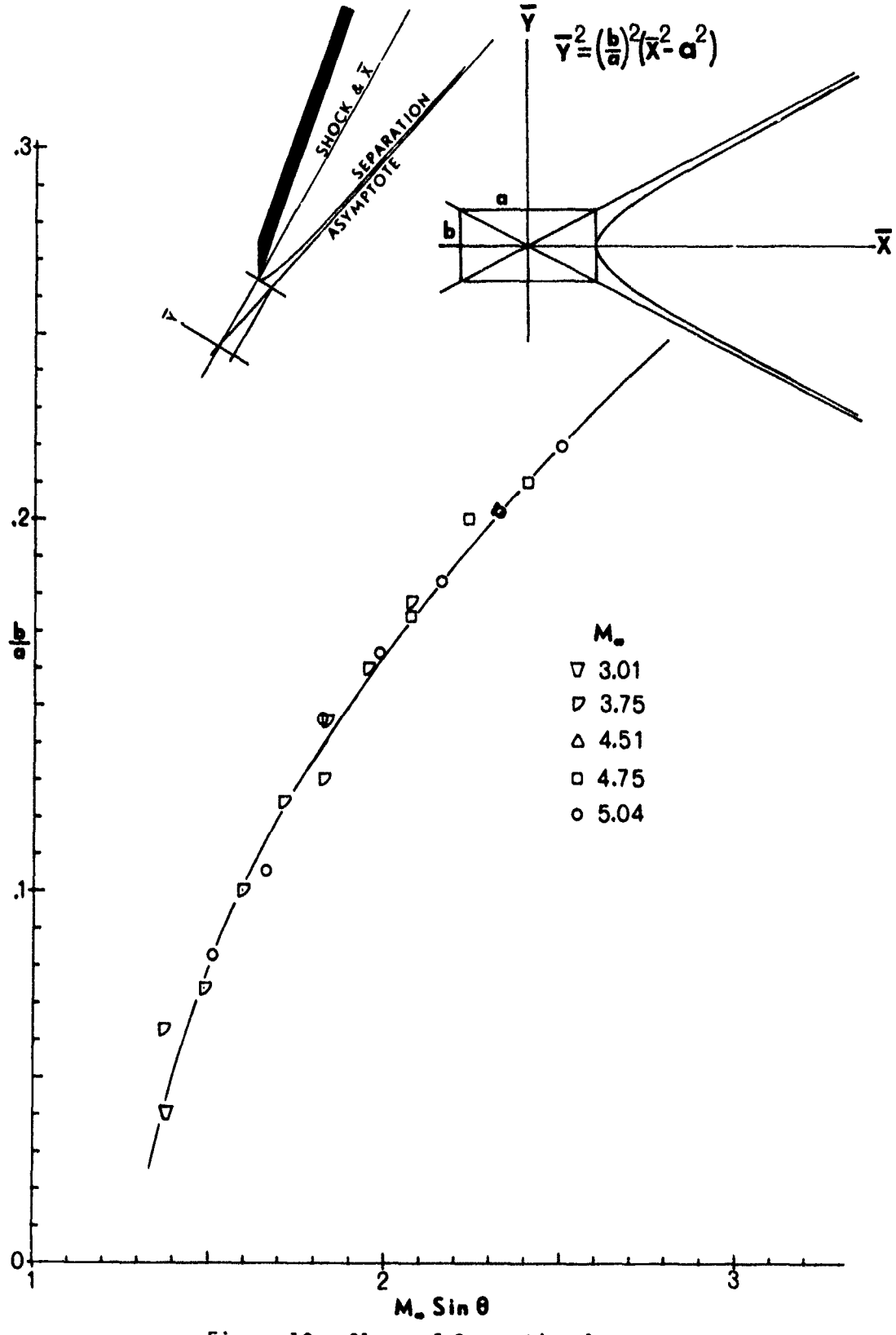

Figure 10. Slope of Separation Asymptote

strengths less than 1.3 the pressure distribution is characterized by a smooth rise from the freestream value to the peak or oblique shock value. The value of either "a" or "b" are more difficult to correlate. Because the slope of the asymptotes is so small the variation of "a" is large with small changes in b/a. Figure 11 shows the correlation obtained for "a" as a function of M_∞ Sin θ. As M_∞ Sin θ approaches 1.3 "b/a" approaches zero and "a" approaches infinity. This infers that the condition for incipient separation is that M_∞ Sin θ equal 1.3. Korkegi's (Reference 13) incipient separation condition was

$$M_\infty \alpha_{inc.} = 0.3 \tag{4}$$

If the incipient separation condition M_∞ Sin θ = 1.3 is transformed to Korkegi's form the results are

$$\text{for } 3 \leq M_\infty \leq 6 \qquad 0.423 \leq M_\infty \alpha_{inc.} \leq 0.438 \tag{5}$$

Equation 5 then predicts separation at a slightly higher fin deflection then Equation 4.

Figure 12 presents the separation coordinates as a function of M_∞ Sin θ. These curves were generated using curve fits of Figures 10 and 11, and the equation

$$\bar{Y}^2 = \left(\frac{b}{a}\right)^2 (\bar{X}^2 - a^2) \tag{6}$$

5. ONSET OF PRESSURE RISE

The point of onset was defined in Section I-1 by the point in the oil flow data at which the undisturbed surface streamlines first begin to curve. This point may be located on the pressure profiles by fairing a line through the pressure rise to the point of separation. As shown in Figure 1 the point at which this line intersects P/P_{FP} = 1 is taken as the point of onset. Having calculated the location of separation as shown in Section II-4 the location of onset may be calculated by correlating the dP/dY from onset to separation. The magnitude of dP/dY was observed to be a function of shock strength and distance aft of the fin leading

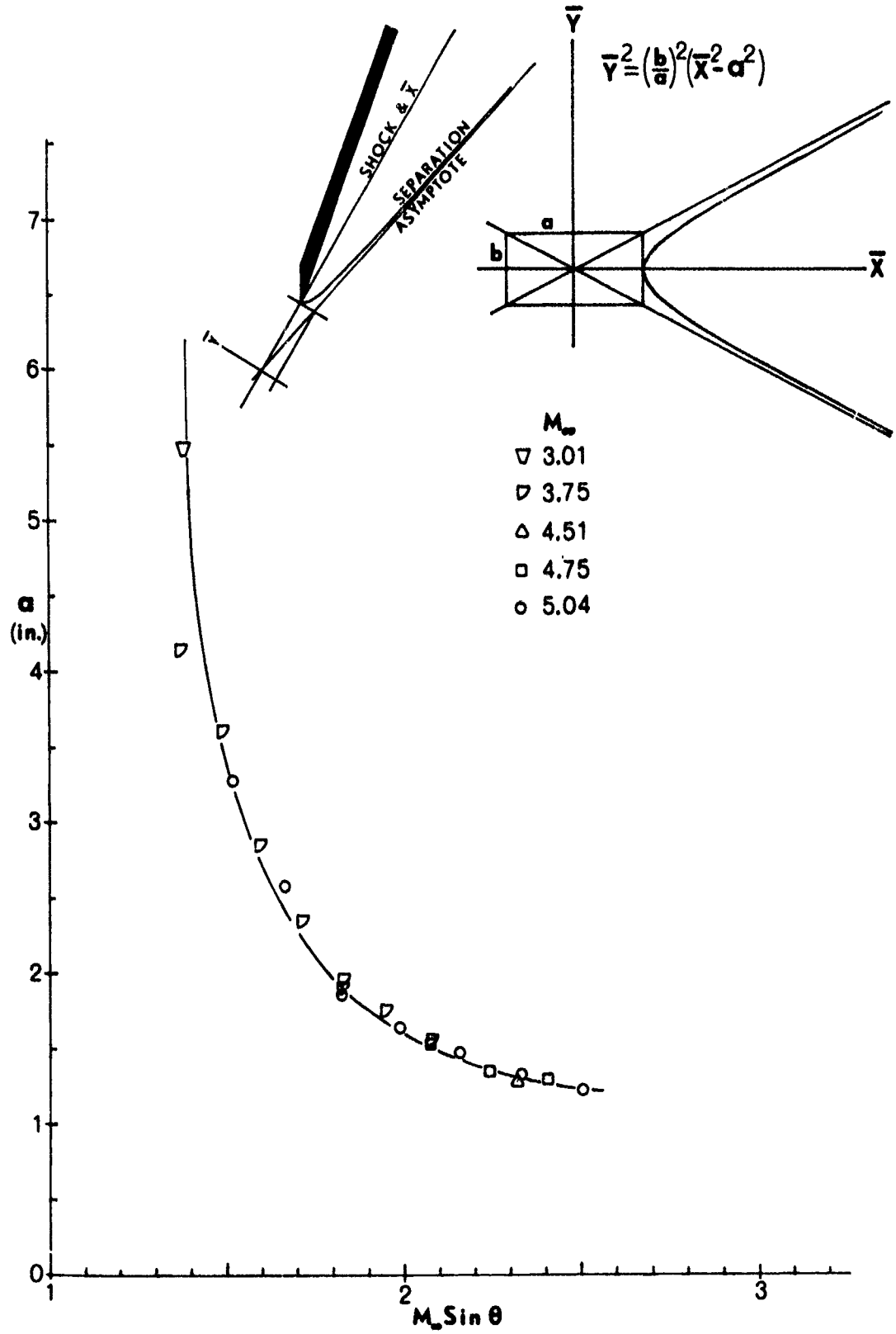

Figure 11. Separation Asymptote Parameter "a"

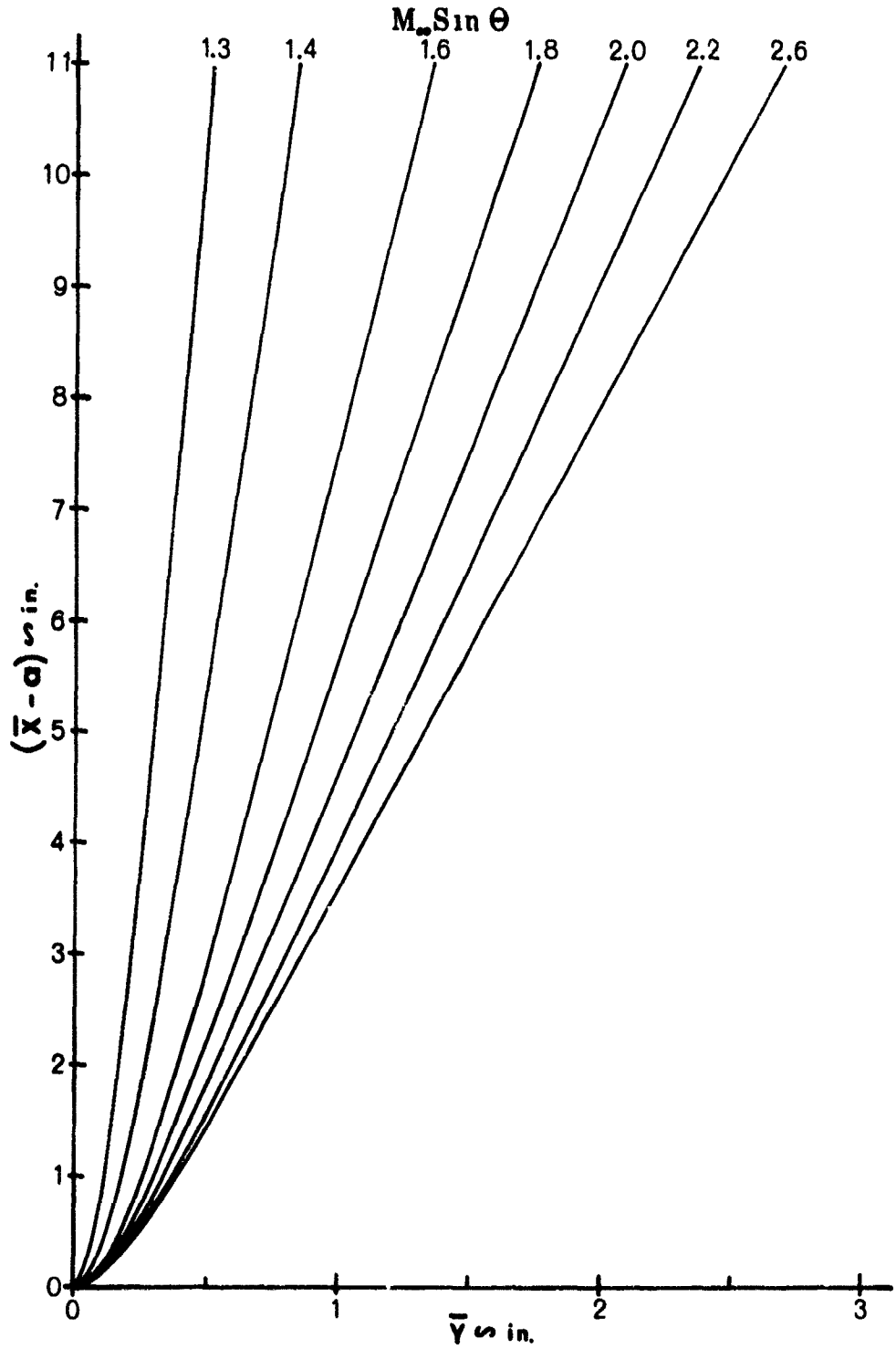

Figure 12. Separation Coordinates as a Function of M_∞ Sin Θ

edge. As shown in Figures 13 to 17 $\Delta P/\Delta Y$ was plotted as a function of M_∞ Sin θ for each Mach number where sufficient data were available. $\Delta P/\Delta Y$ is found to be a linear function of shock strength at each station within the interaction region. The slope of this function is dependent on distance aft of the fin leading edge and on boundary layer thickness as shown in Figure 18. When constructing a pressure profile like the one shown in Figure 1 the location of onset is determined by first locating separation and then extending the profile to onset using an estimation of $\Delta P/\Delta Y$ from Figure 18.

6. PRESSURE DISTRIBUTIONS

Discussion of the pressure distributions will be confined to data taken at shock strengths greater than M_∞ Sin θ = 1.3. These are characterized by the vortex dominated flow where the peak pressure is greater than the oblique shock values, a trough is observed at the shock location, and a distinct plateau region exists. Because of the complexity of the 3-D interaction the pressure distributions must be broken up into several sections for any correlation to be obtained.

The pressure distribution is first separated into two main parts by the shock wave. The inner region consists of a smooth and sharp rise from the shock pressure to the peak value near the fin. No correlation with 2-D data has been found here. The outer region however has distinct 2-D characteristics as described in Sections II-3 and II-4. This outer region, extending from onset to the shock location, is divided into two subregions by the point of boundary layer separation. The pressure distribution corresponds to that of a 2-D interaction of equal shock strength.

a. Inner Region

The normalized coordinates for plotting the distribution in the inner region are

$$\frac{P - P_{SH}}{P_{PK} - P_{SH}} \quad \text{and} \quad \frac{Y - Y_{SH}}{Y_{PK} - Y_{SH}}$$

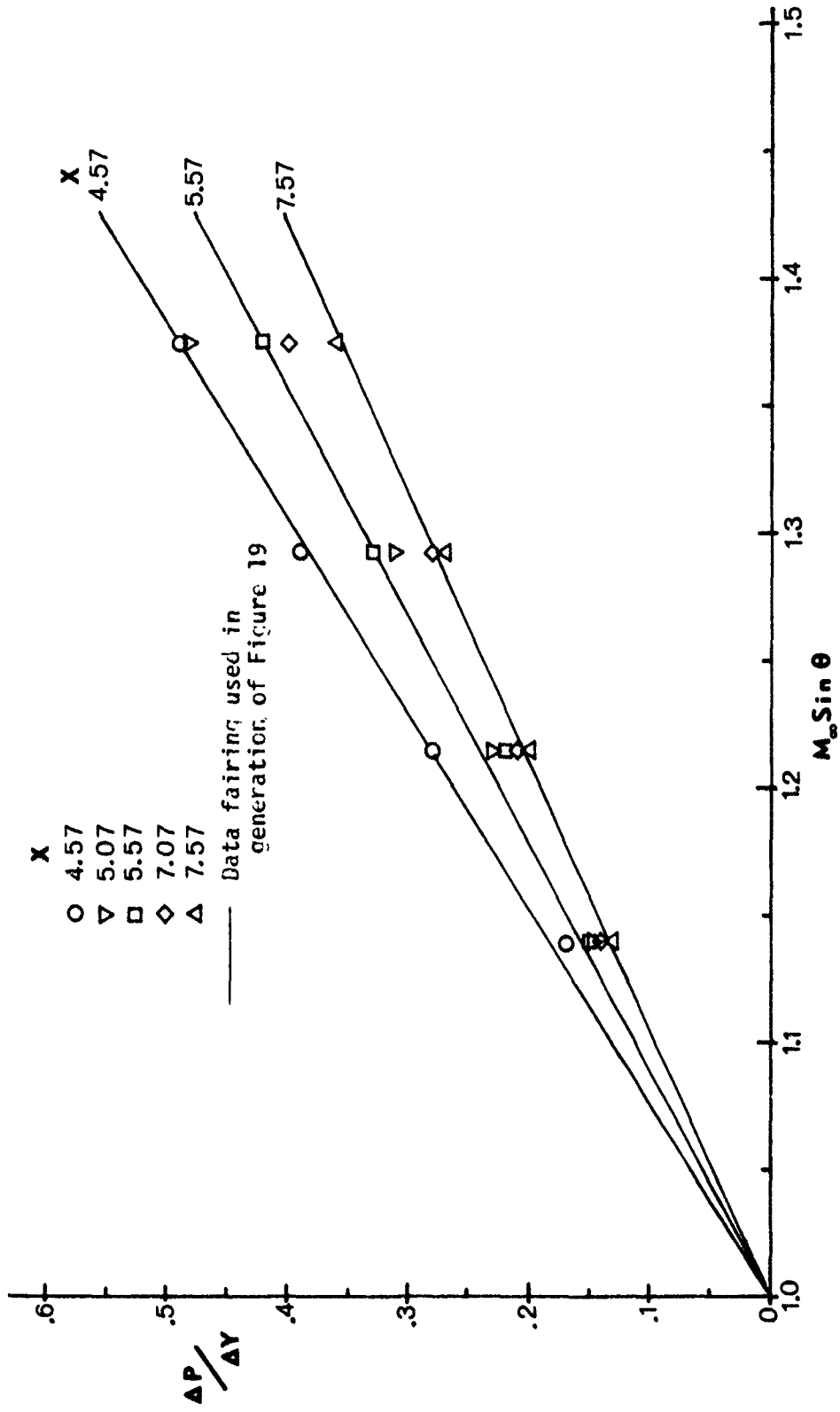

Figure 13. Onset Pressure Gradient at Mach 2.95

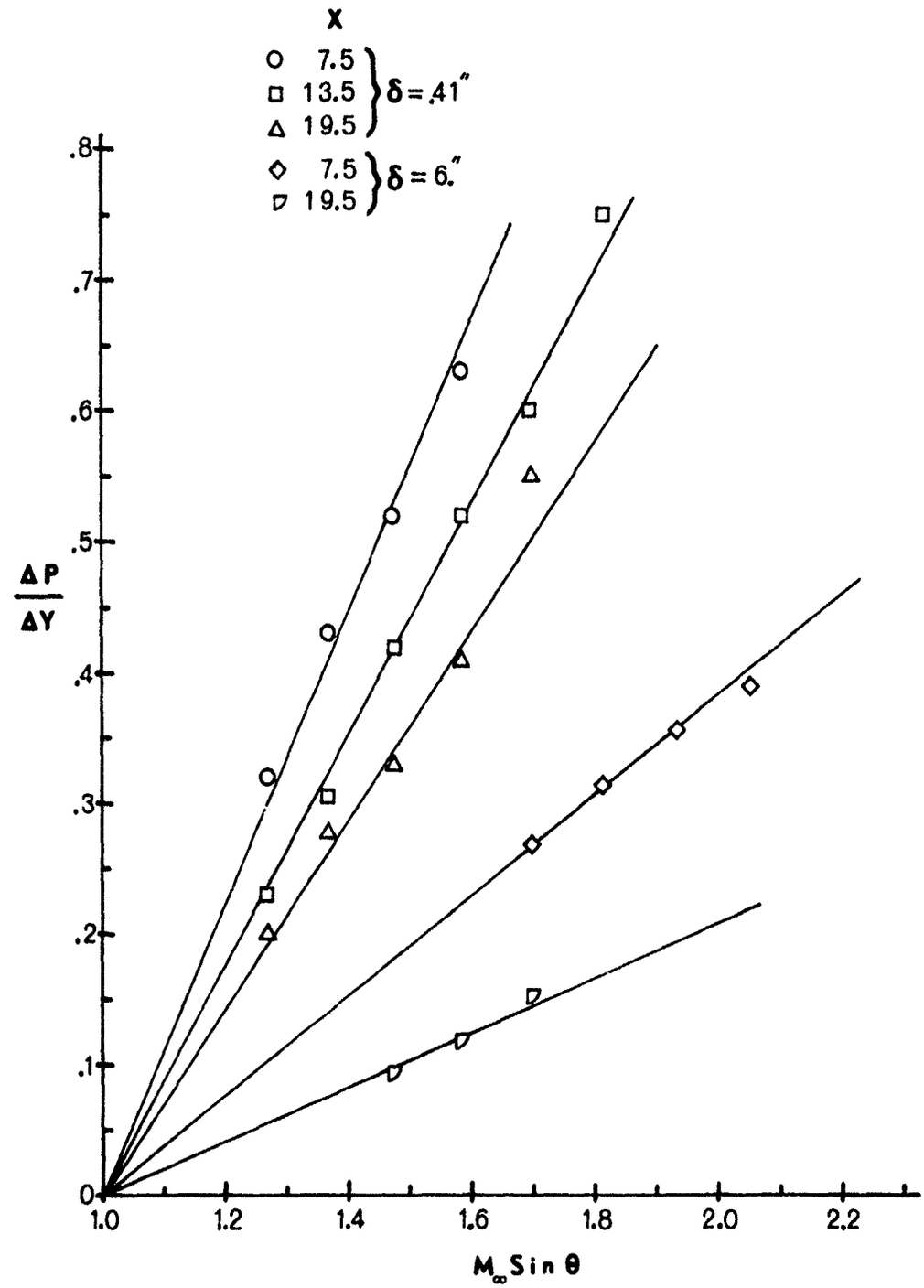

Figure 14. Onset Pressure Gradient at Mach 3.71

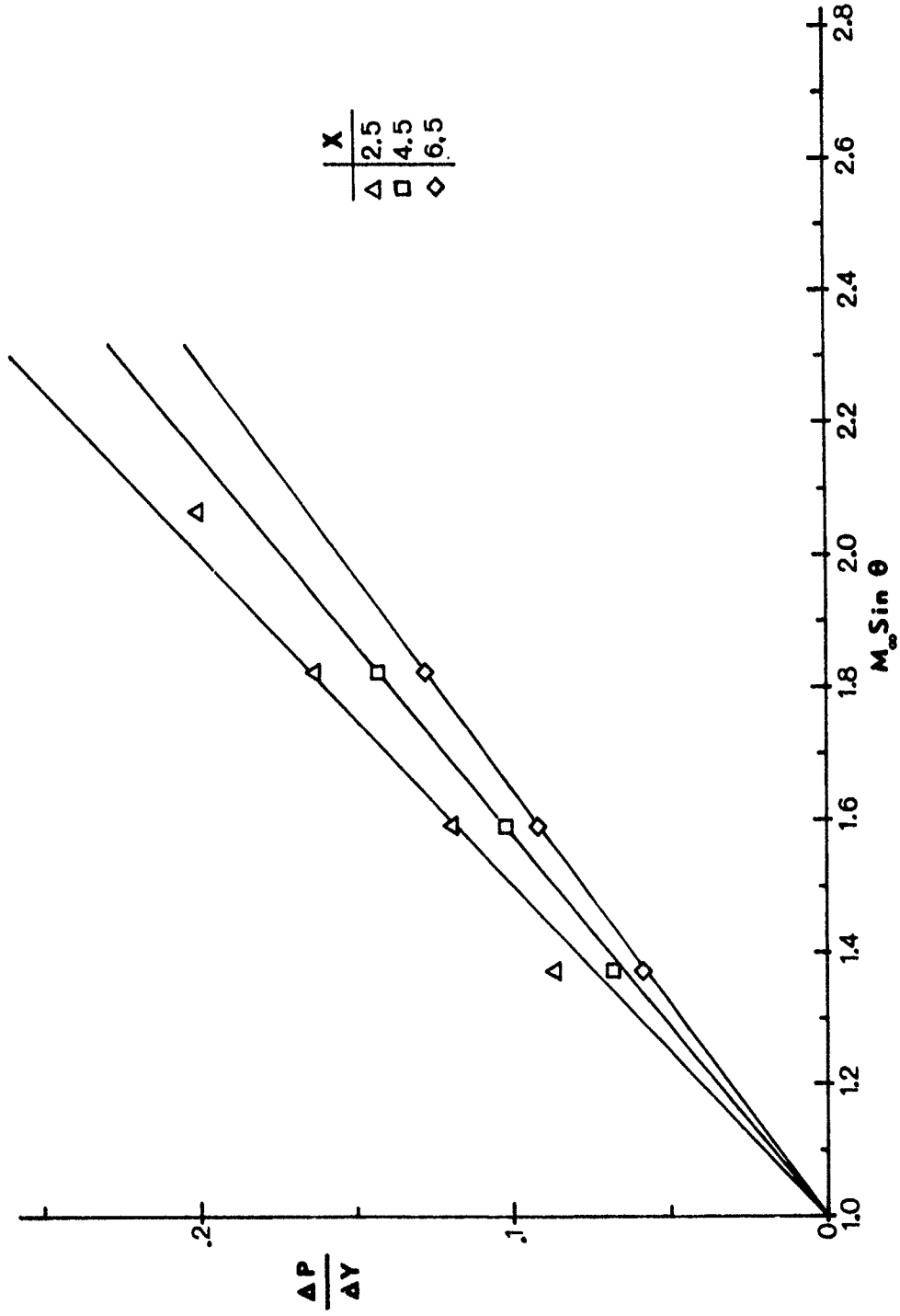

Figure 15. Onset Pressure Gradient at Mach 3.75

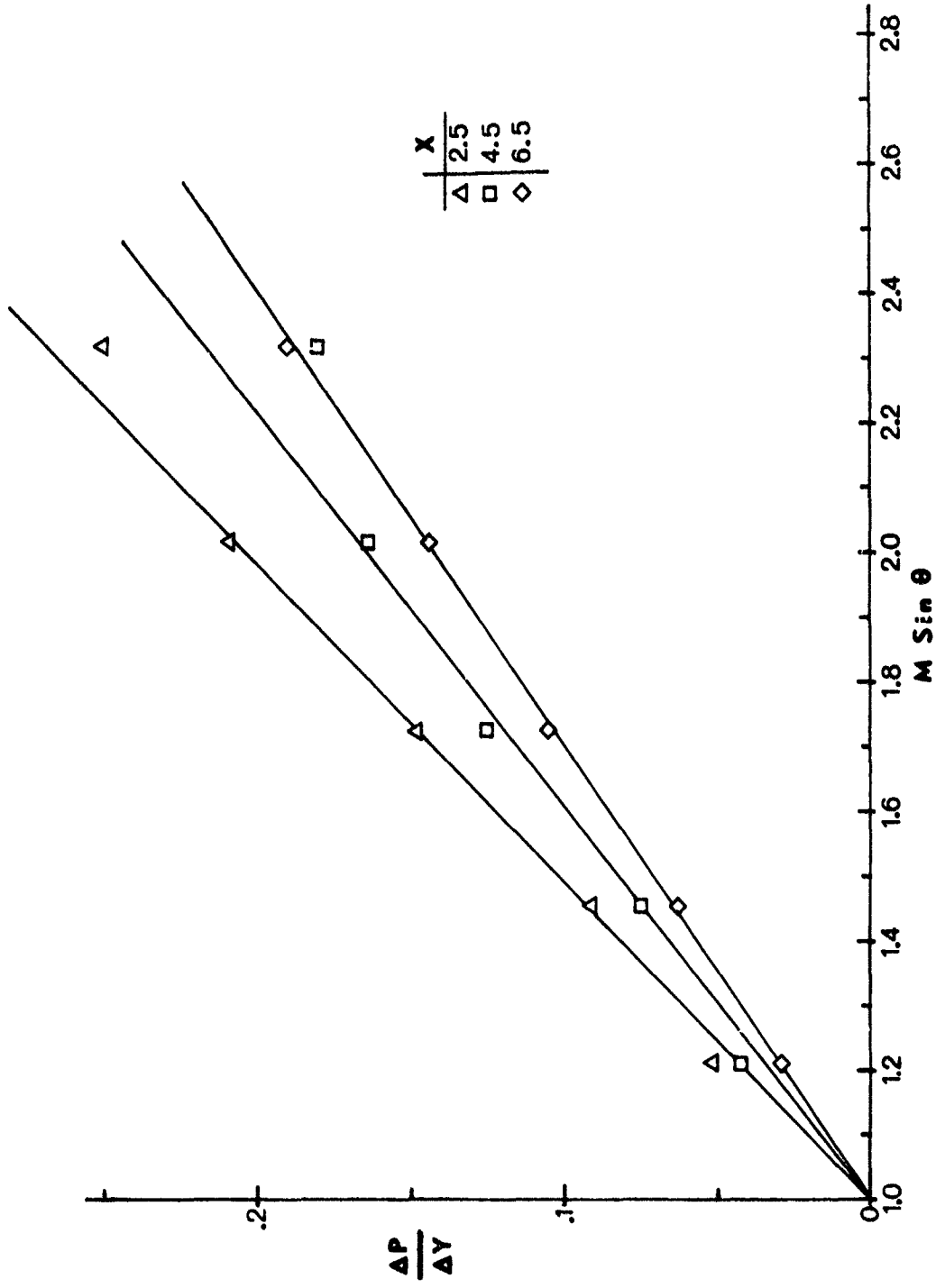

Figure 16. Onset Pressure Gradient at Mach 4.51

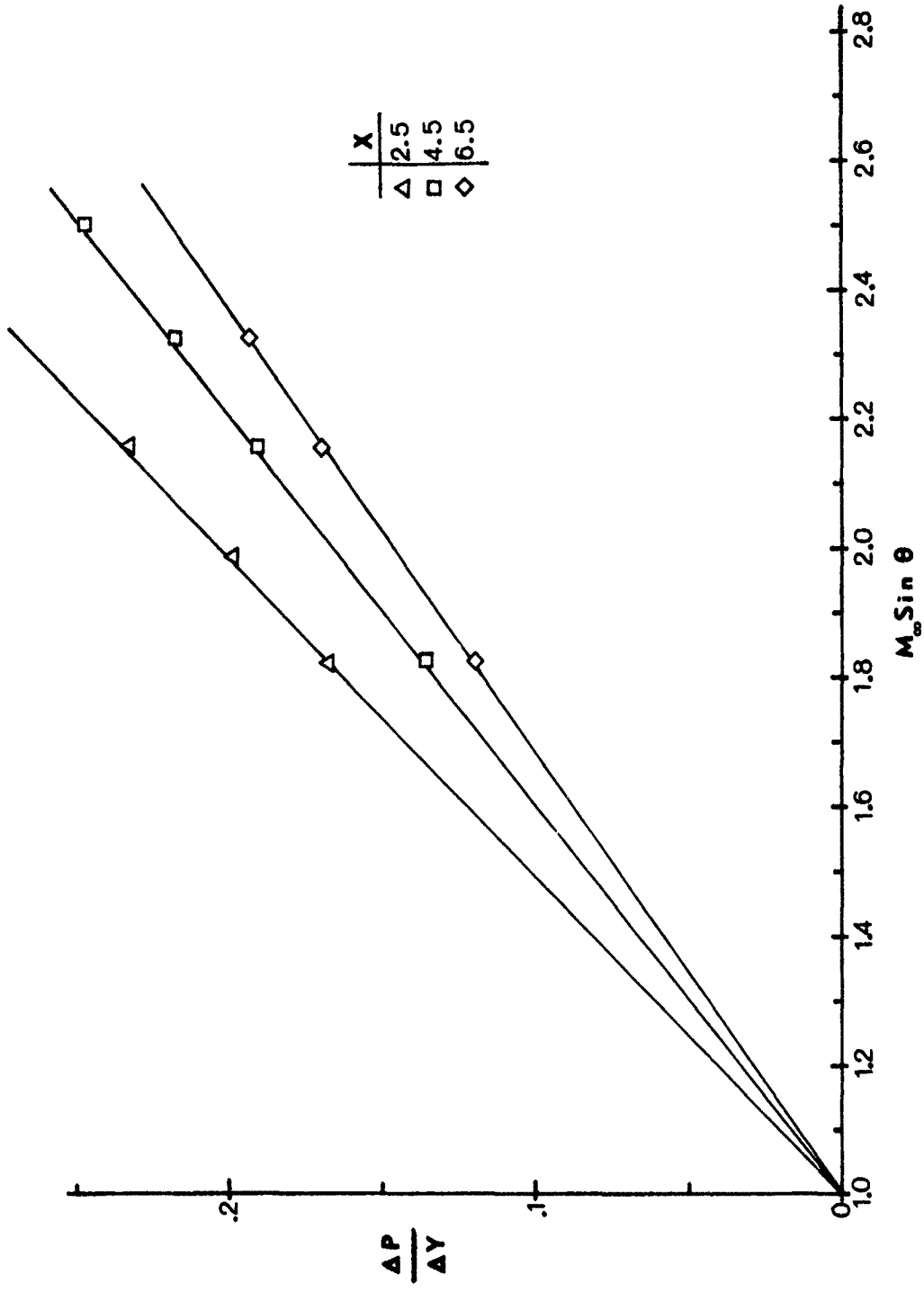

Figure 17. Onset Pressure Gradient at Mach 5.04

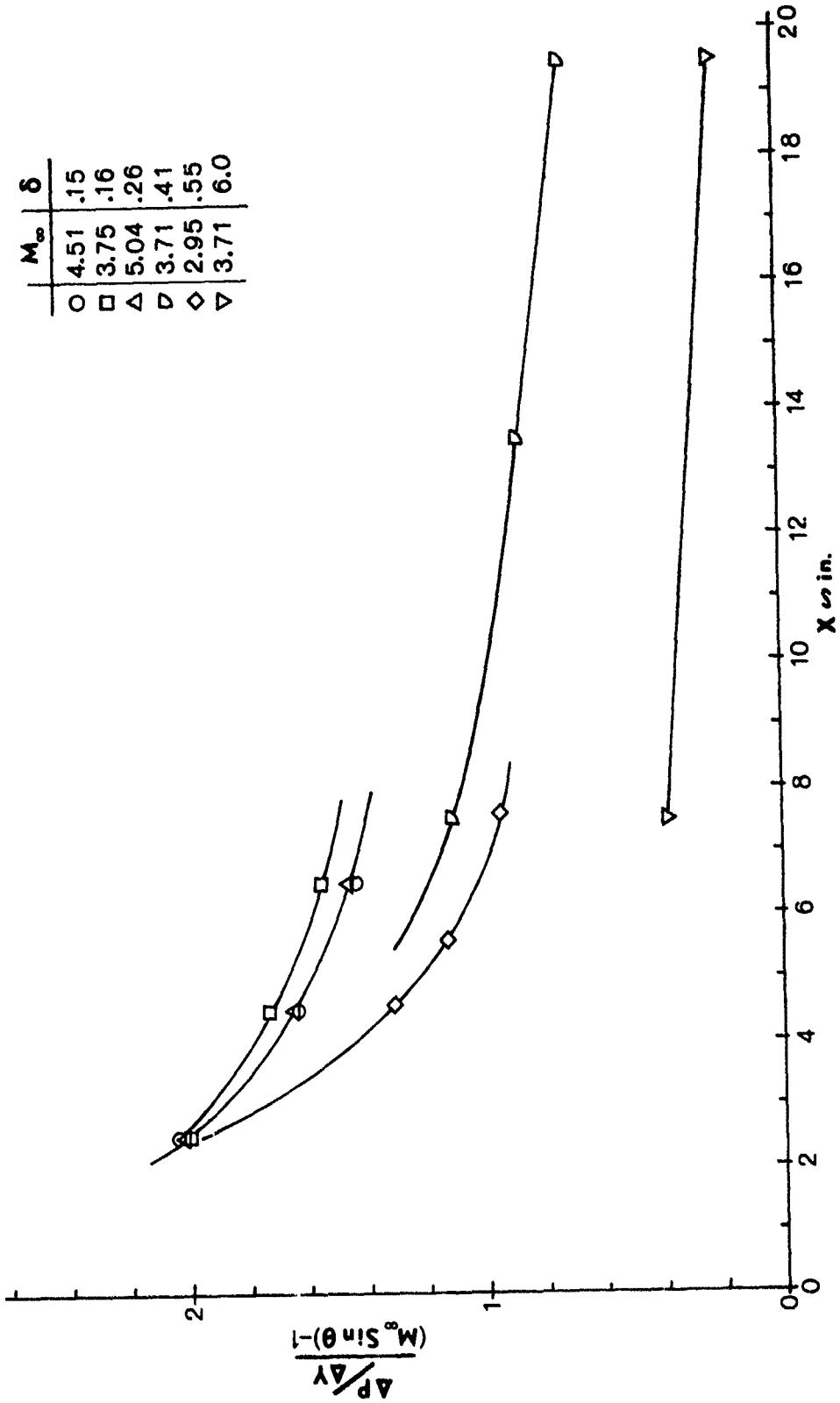

Figure 18. Onset Pressure Gradient Correlation

Figure 19 presents the correlation for the inner region pressure distribution. Data scatter is obvious and to be expected from such an elementary correlation method. However the peak pressure and its location can be accurately determined from Figures 3 and 4 and Figure 19 is then adequate for producing a fast and simple engineering approximation to the distribution between the peak and the shock.

b. Outer Region

The outer region which extends from the shock wave to onset is divided into two subregions. Subregion 1 extends from the shock to the separation line. The normalized coordinates employed in correlating the data in this subregion are

$$\frac{P - P_{FP}}{P_{PL} - P_{FP}} \quad \text{and} \quad \frac{Y_{SEP} - Y}{Y_{SEP}}$$

Figure 20 presents the pressure distribution in this subregion. The data correlation is good only to $(Y_{SEP} - Y)/Y_{SEP} = 0.32$ which may be used as the location of the plateau for engineering purposes. Between the plateau and the shock, the pressure distribution is a strong function of shock strength. At $M_\infty \sin\theta \simeq 1.3$ the pressure remains fairly constant between the plateau and shock locations. As $M_\infty \sin\theta$ increases the pressure begins to fall off into a trough at the shock which deepens with $M_\infty \sin\theta$ and X.

Subregion 2 extends from the separation line to the onset of the interaction region. The normalized coordinates employed in the data correlation were

$$\frac{P - P_{FP}}{P_{PL} - P_{FP}} \quad \text{and} \quad \frac{Y - Y_{SEP}}{Y_{ON} - Y_{SEP}}$$

The correlation is shown in Figure 21. The point of onset may be measured from oil flow data at the point where the freestream surface streamlines first begins to curve or it can be calculated from Figure 18.

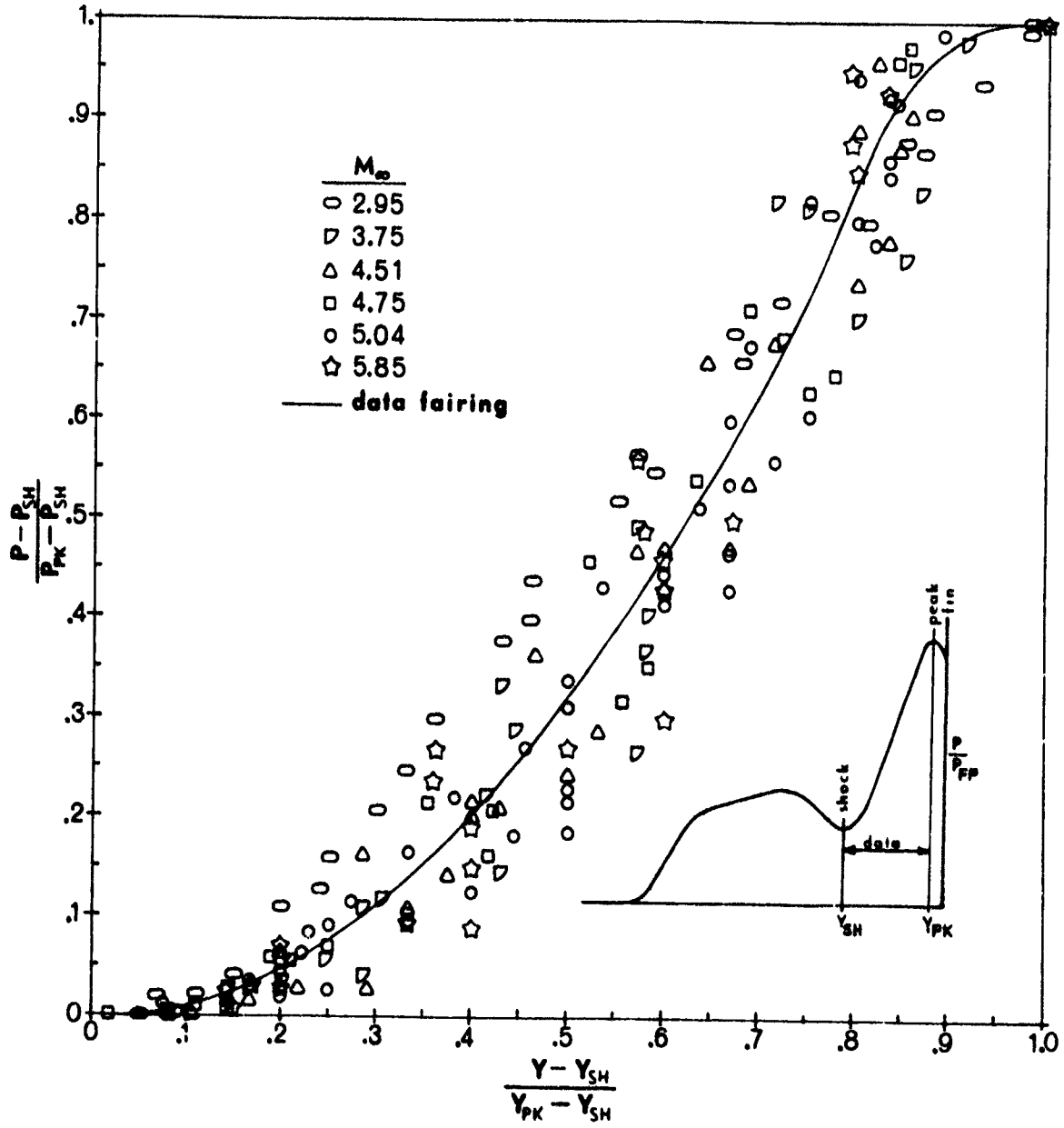

Figure 19. Pressure Distribution, Peak-to-Shock

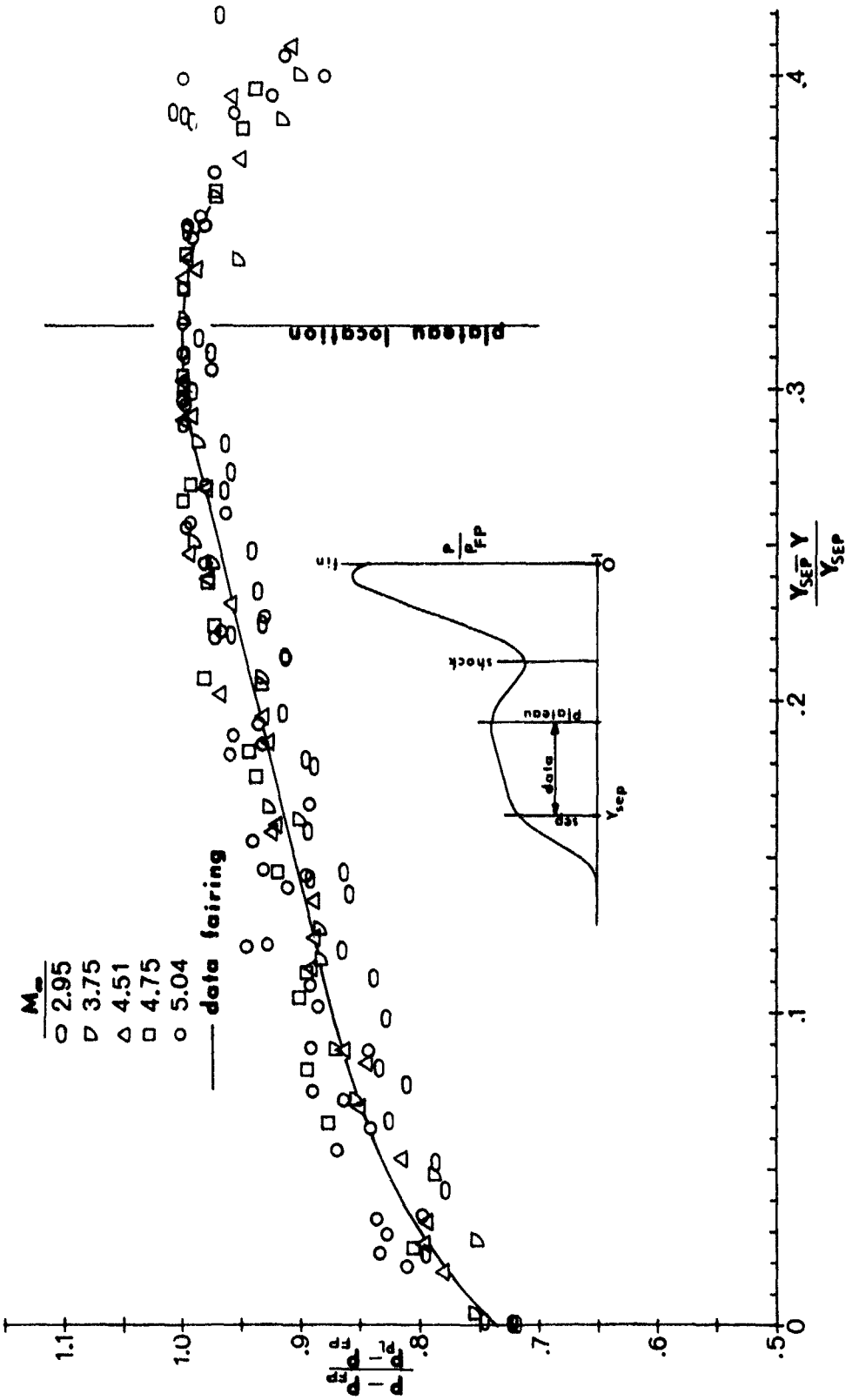

Figure 20. Pressure Distribution, Plateau-to-Separation

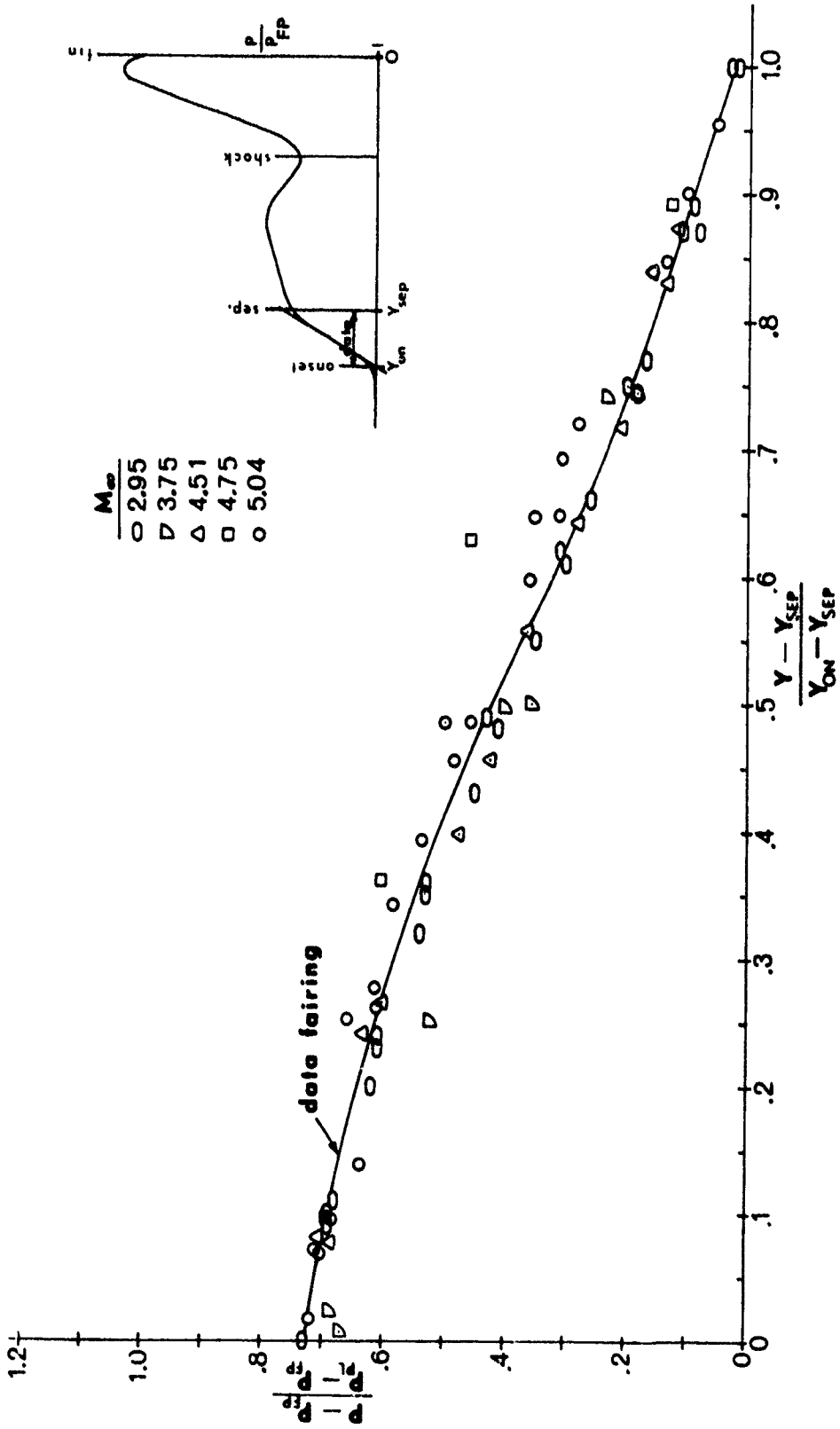

Figure 21. Pressure Distribution, Separation-to-Onset

The pressure distribution has been correlated from onset to the plateau and from the shock to the peak location. Work is still required to increase the utility of Figures 6 and 18 by additional data, however the characteristics important from an engineering standpoint have been defined. These are the location and magnitude of the pressure at separation, at the plateau and at the peak.

SECTION III

HEAT TRANSFER PROFILES

A typical heat transfer profile was introduced in Section I-1. The dominant characteristics are a small peak at the line of separation followed by a nearly linear rise to the shock location. At the shock a sharp change in slope occurs and the heating rates continue to rise to the large inner peak.

1. PEAK HEAT TRANSFER

It was shown in Section II-1 that the peak pressure data taken in flows having large differences in boundary layer thickness could be correlated through the term "X/δ". This type of correlation has been observed to hold for the peak heating data as well. Figures 22 to 29 present the peak heating data for boundary layer thicknesses up to 6 inches. At each station downstream of the fin leading edge the peak Stanton number correlates linearly with shock strength for a given boundary layer thickness. The slope of a line faired through the data correlates with "X/δ" as in the peak pressure correlations. This data fairing has been passed through the point $\left(\frac{St_{PK}}{St_{FP}}, M_\infty \sin\theta\right) = (0.75, 1)$ in all data sets because it provides a simple yet accurate data fit for $M_\infty \sin\theta > 1.3$. At small $M_\infty \sin\theta$ the data actually approach (1, 1). The only exception to this data trend appears in the Mach 2.95 data (Reference 14) in which the data tend to follow a line originating from point (1, 1) even at $M_\infty \sin\theta > 1.3$. No explanation for this difference in data trends was established. The expression for the peak Stanton number derived by this method is

$$\frac{St_{PK}}{St_{FP}} = (M_\infty \sin\theta - 1)\, n_{St} + 0.75 \qquad (7)$$

where n_{st} is a function of X/δ. The function n_{St} is shown in Figure 30.

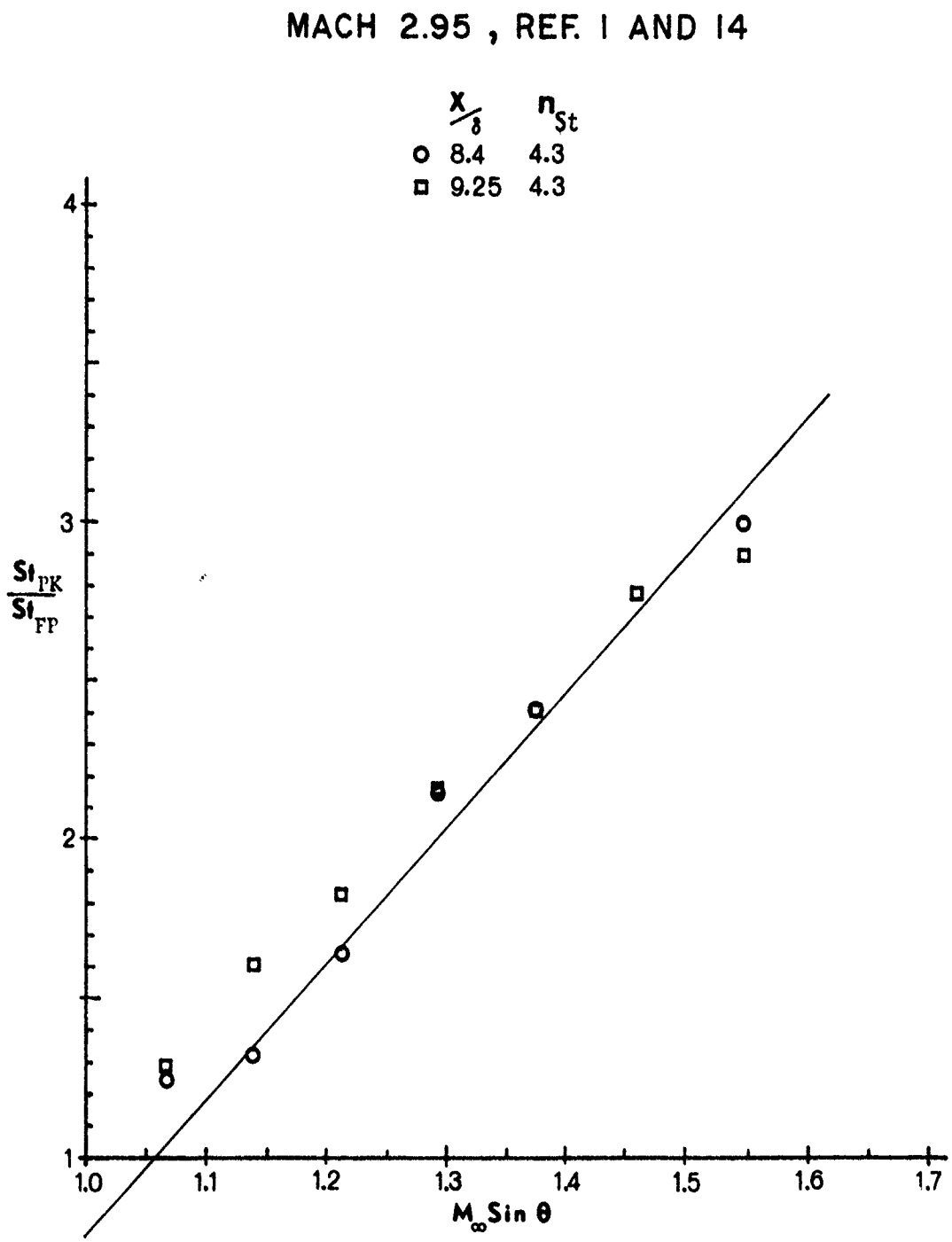

Figure 22. Peak Heating at Mach 2.95

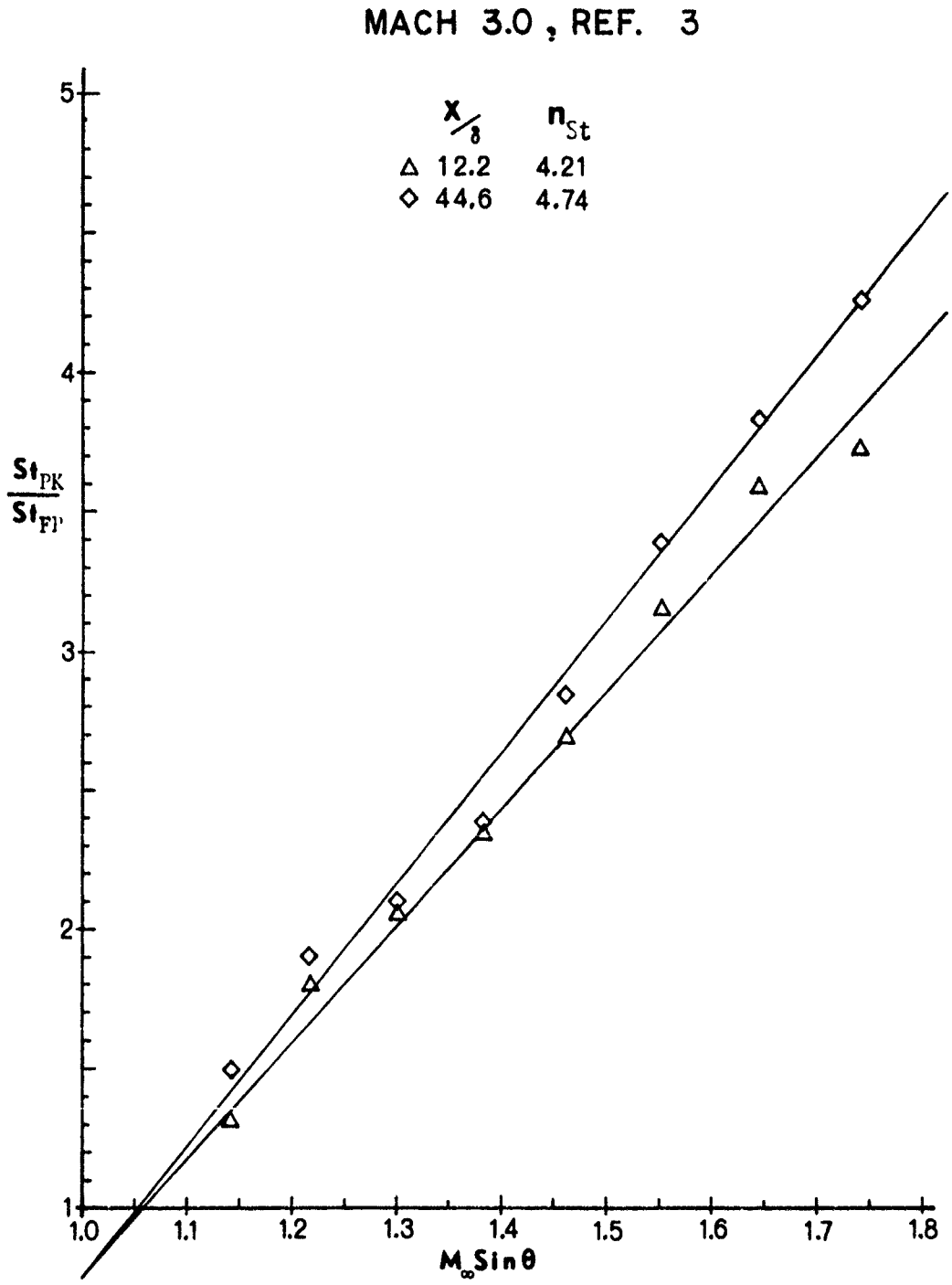

Figure 23. Peak Heating at Mach 3.00

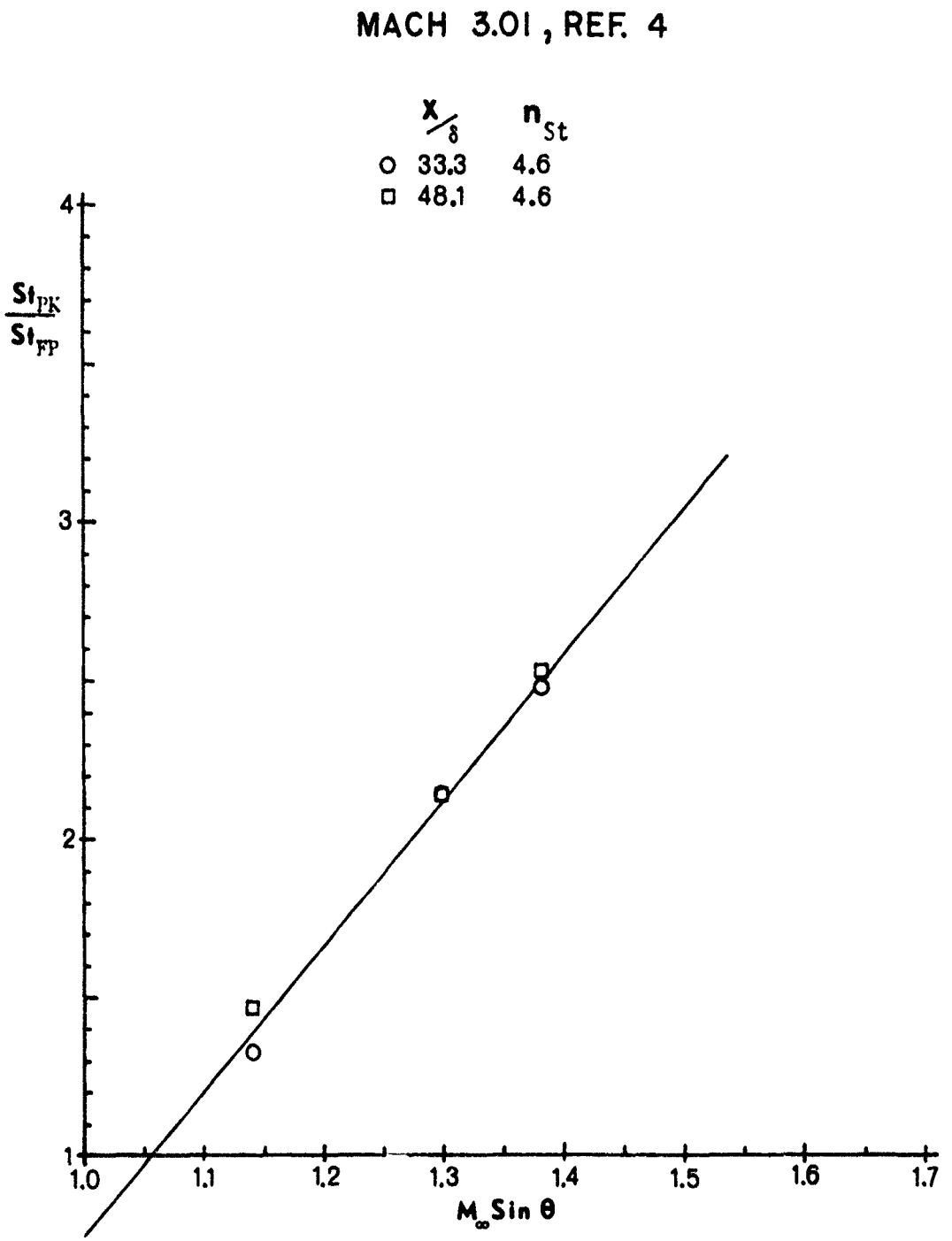

Figure 24. Peak Heating at Mach 3.01

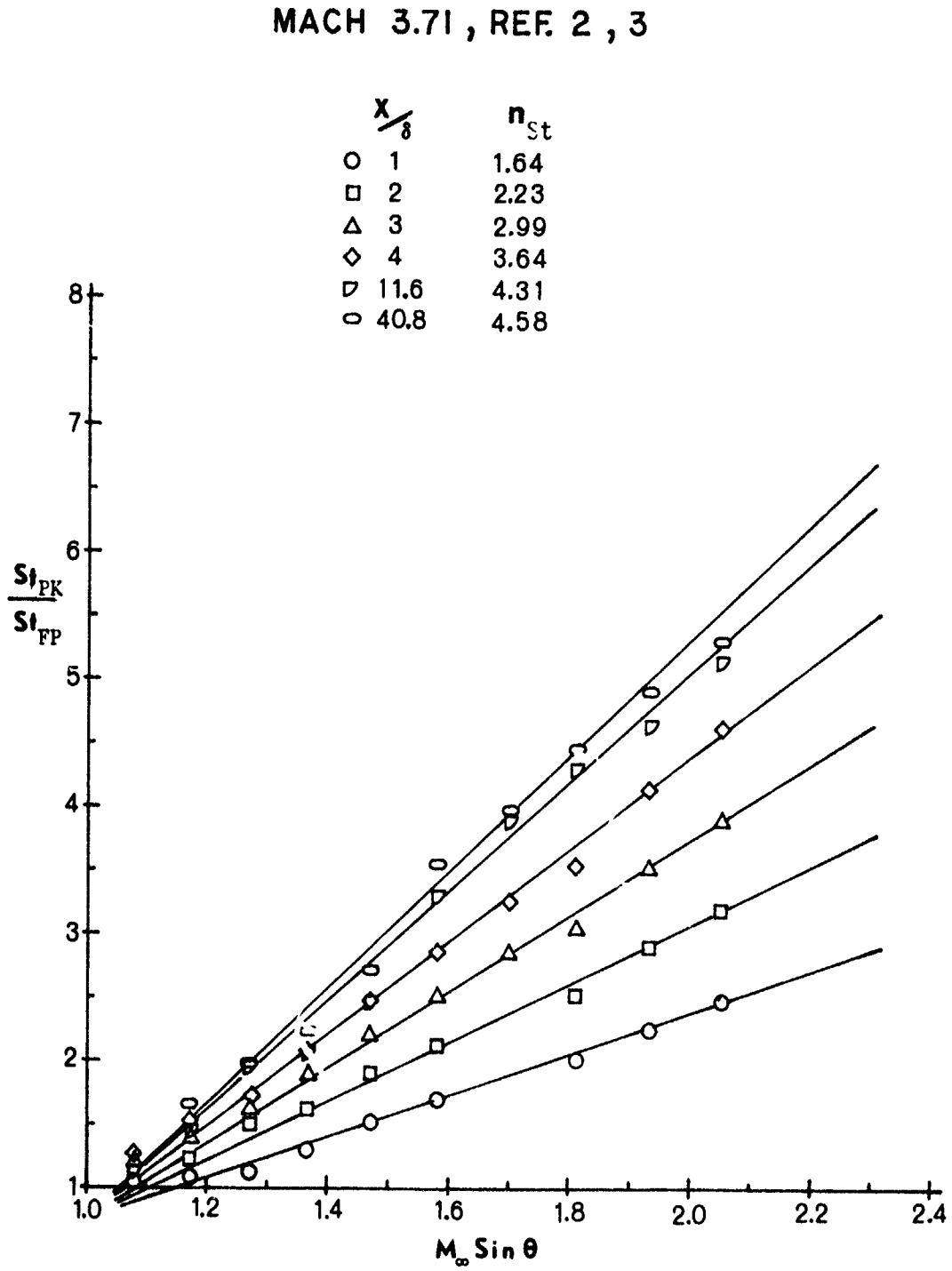

Figure 25. Peak Heating at Mach 3.71

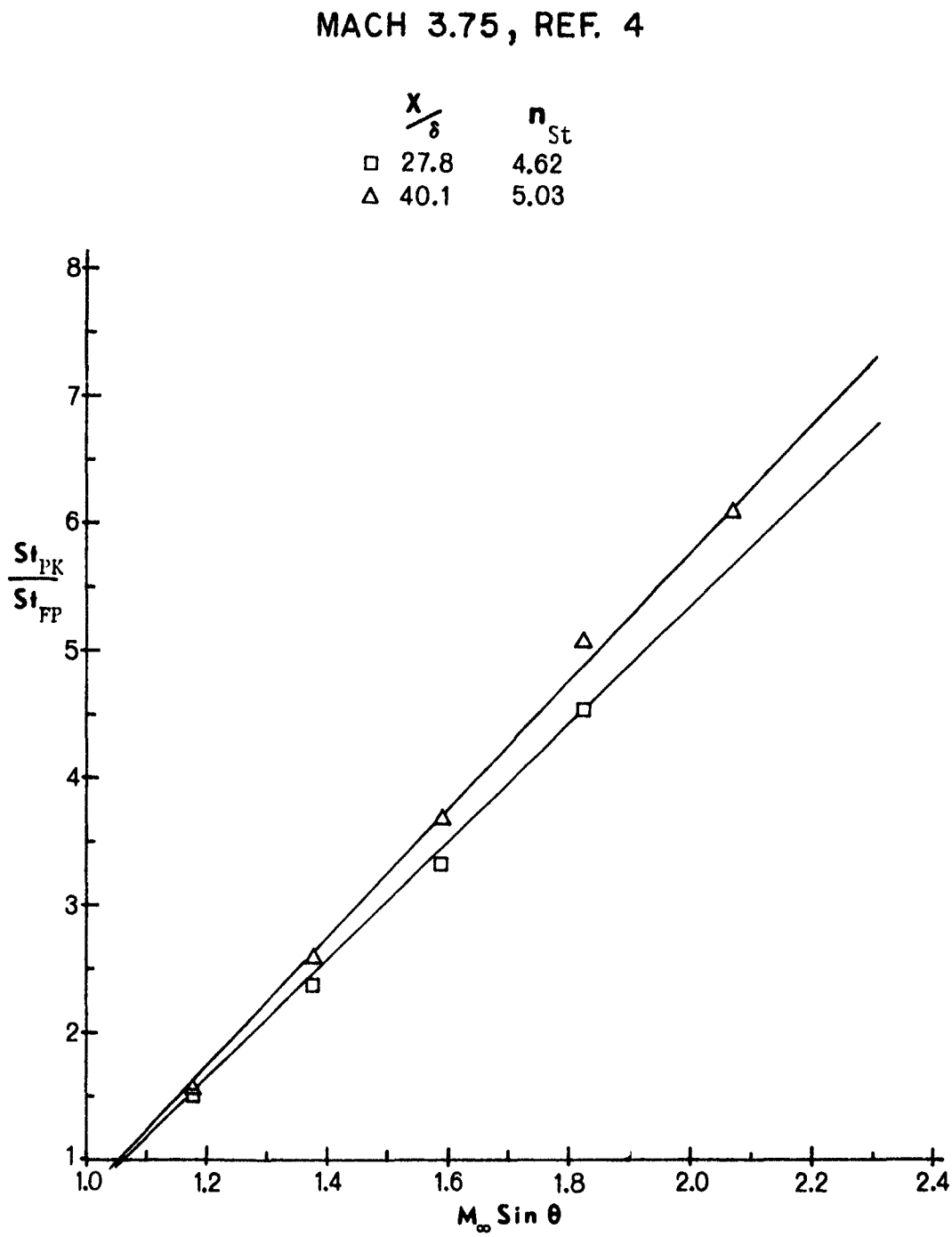

Figure 26. Peak Heating at Mach 3.75

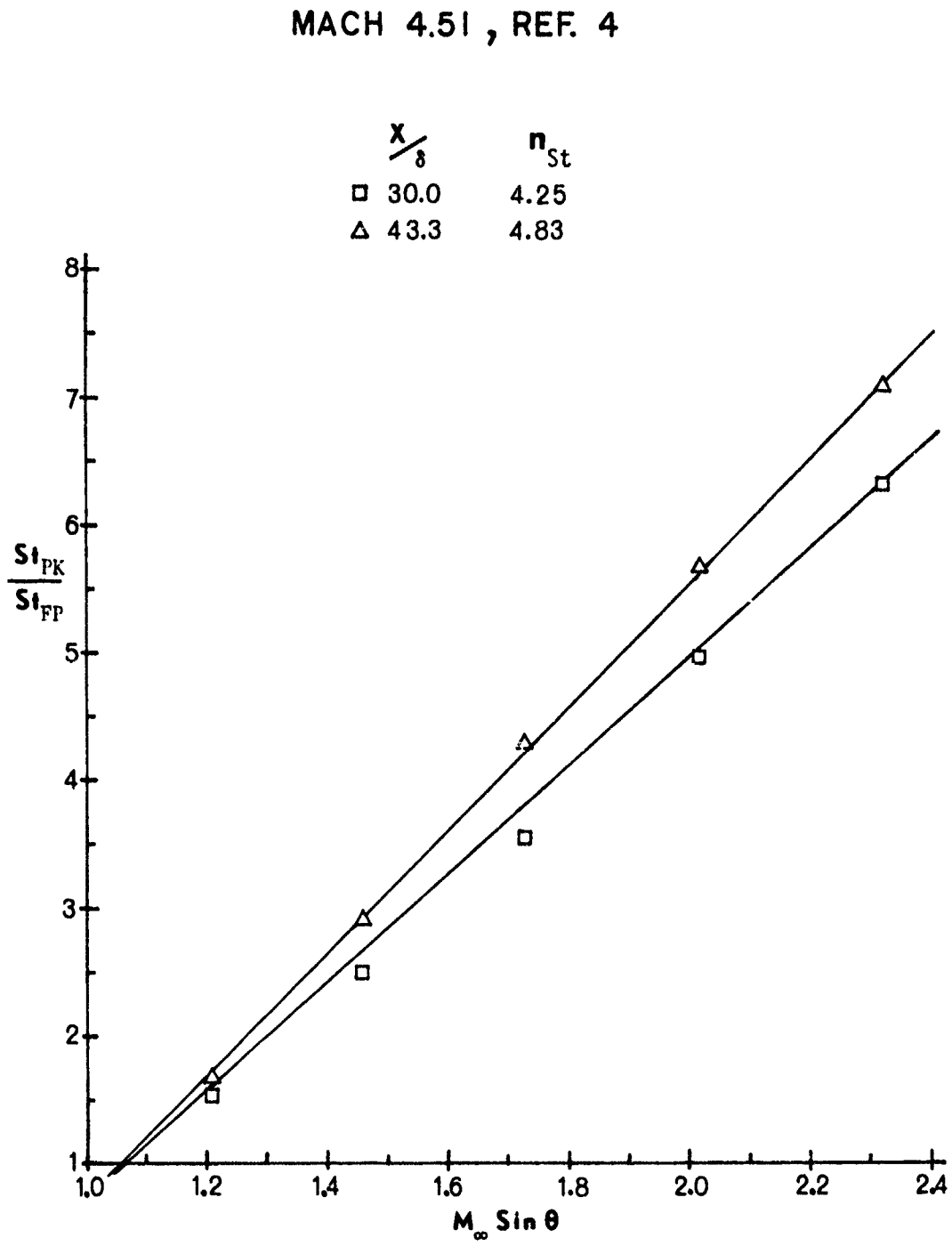

Figure 27. Peak Heating at Mach 4.51

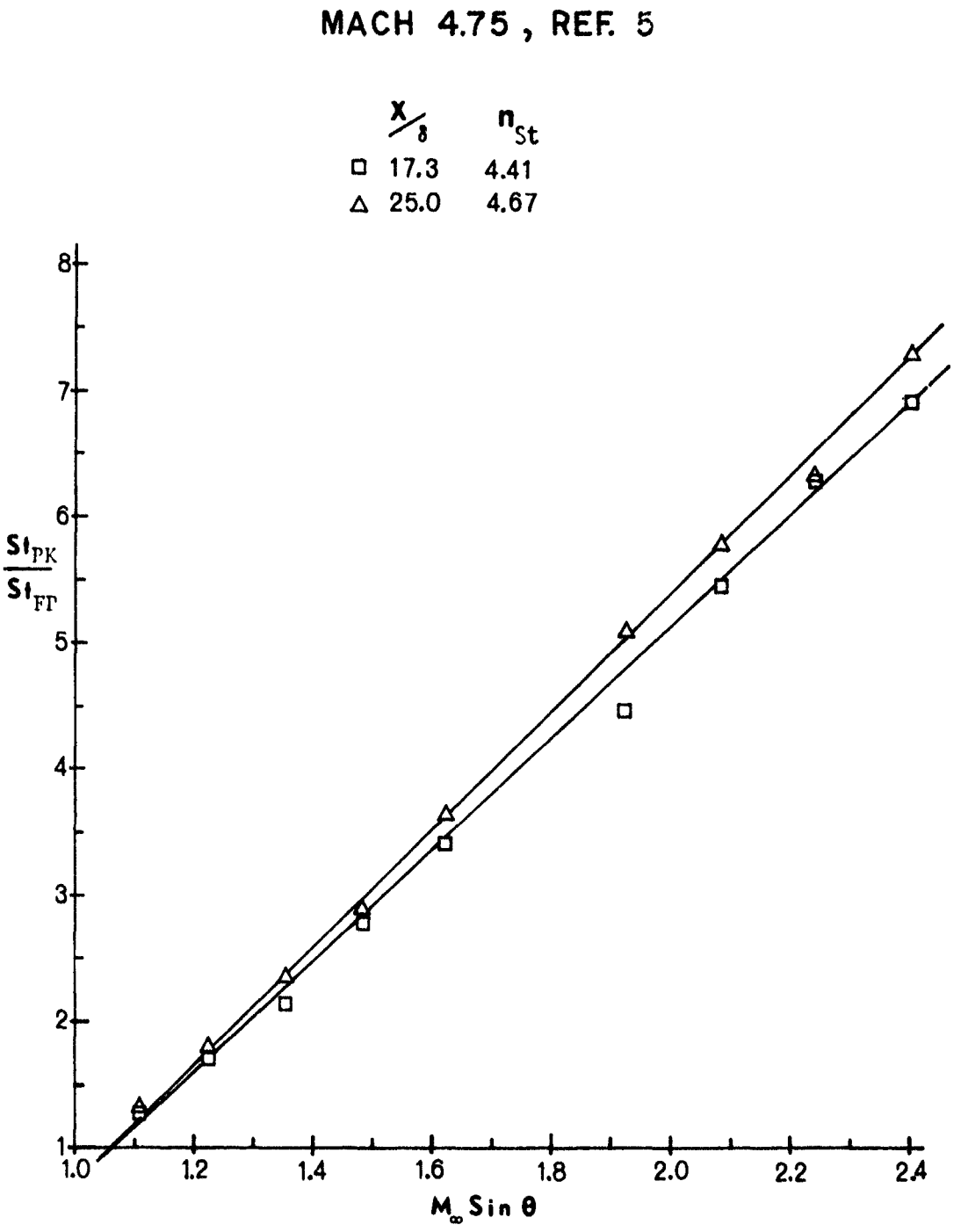

Figure 28. Peak Heating at Mach 4.75

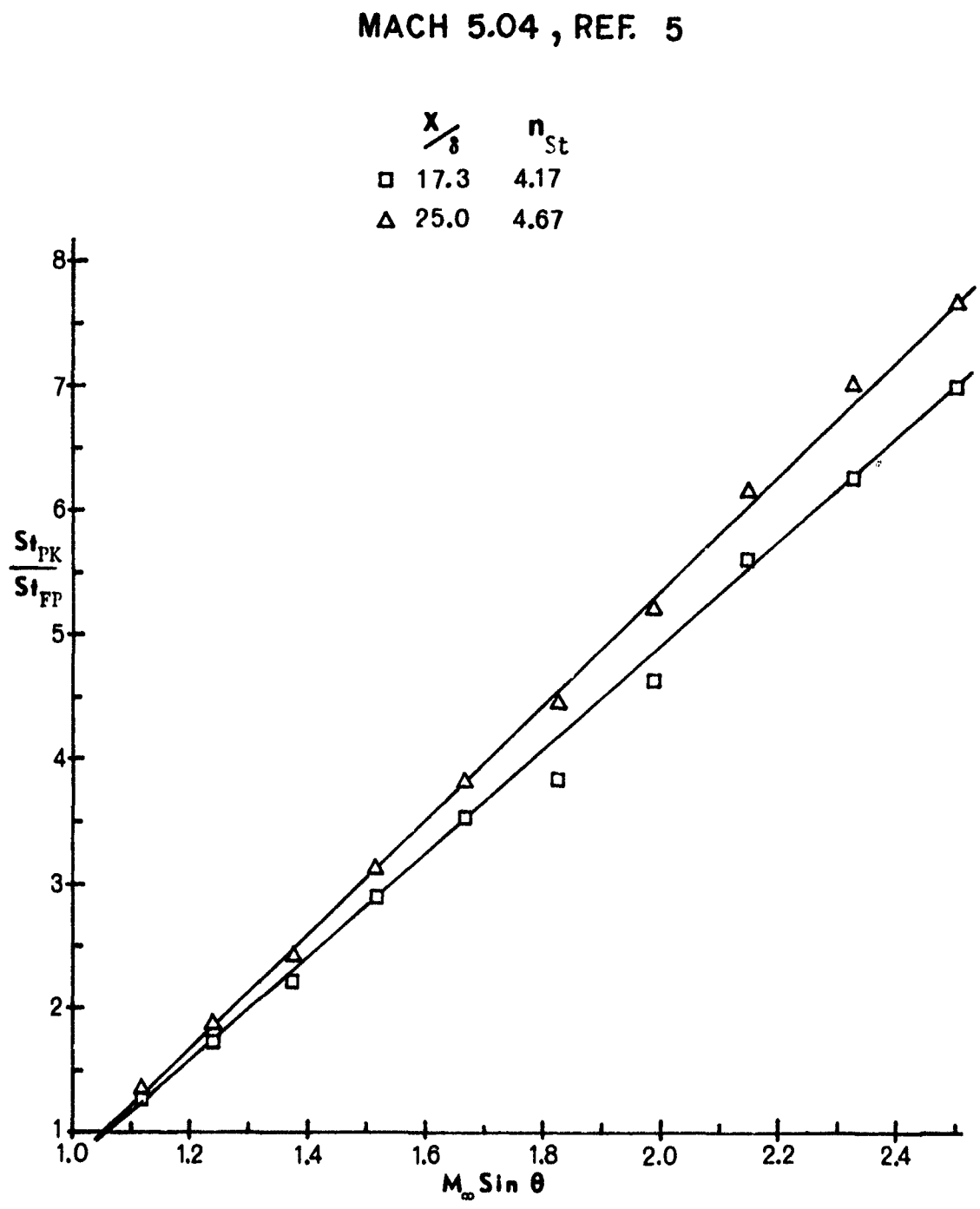

Figure 29. Peak Heating at Mach 5.04

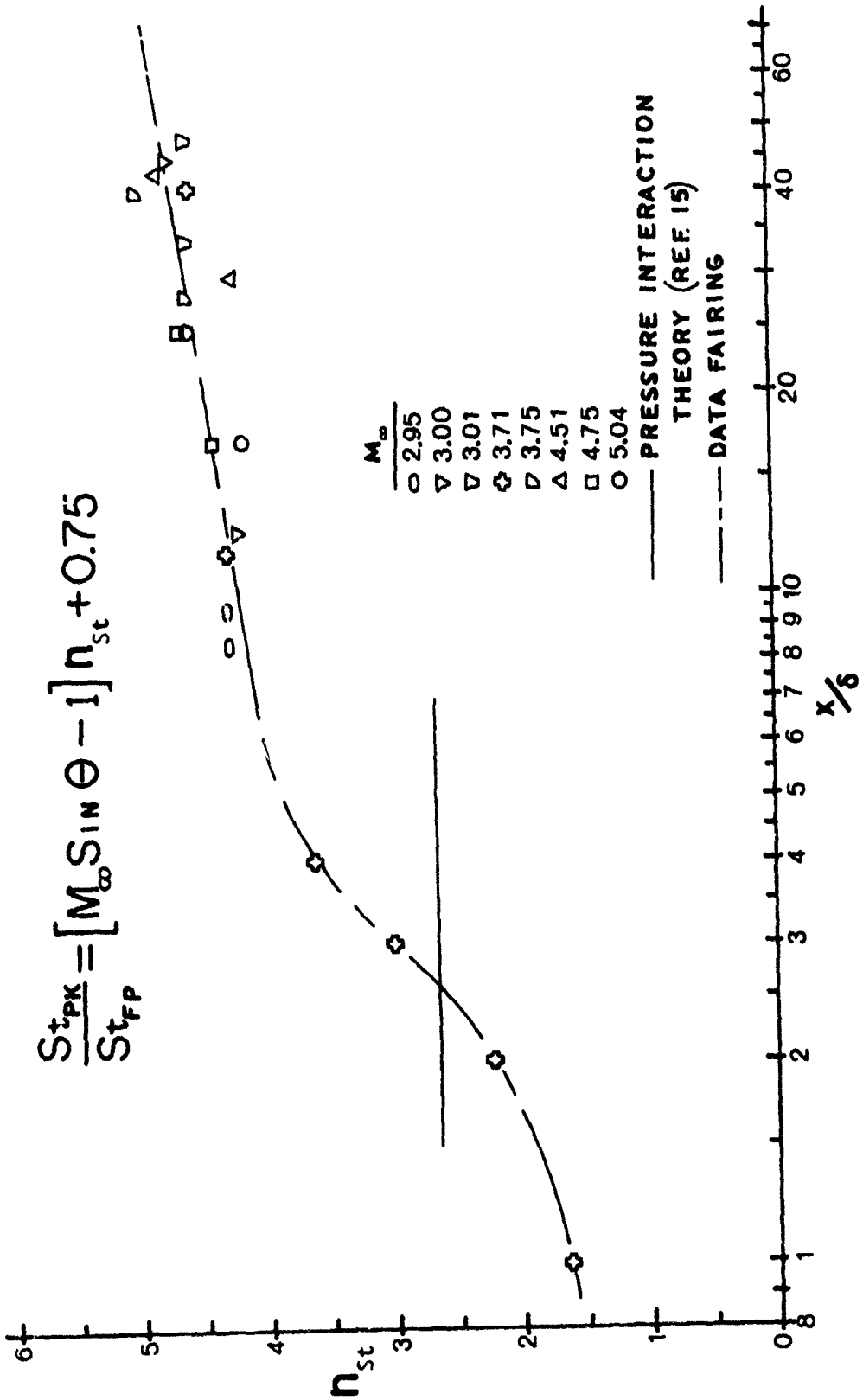

Figure 30. Coefficient in Peak Heating Correlation

Two dimensional interaction data has shown that the peak Stanton number can be correlated with the oblique shock pressure ratio in the form

$$\frac{St_{PK}}{St_{FP}} = \left(\frac{P_2}{P_1}\right)^{0.8} = \left(\frac{7(M_\infty \text{ Sin } \theta)^2 - 1}{6}\right)^{0.8} \tag{8}$$

known as the pressure interaction theory (Reference 15).

By plotting this Stanton number as a function "M_∞ Sin θ" and calculating the slope of the curve a value for n_{St} for 2-D data is derived. This value is also shown on Figure 30. It can be seen that within three boundary layer thicknesses of the fin leading edge the 3-D peak heating rates have exceeded the 2-D values at the same shock strength.

In the 3-D interaction the region downstream of the shock wave contains a vortex which dominates the flow field and is not found in the 2-D interactions. This vortex is the phenomenon which raises the peak heating rates above the 2-D predictions. The vortical amplification factor may be found by dividing the 3-D peak heating rate by the oblique shock pressure ratio raised to the 0.8 power. This amplification factor was calculated using the 3-D peak heating correlation of Figure 30 and oblique shock relations.

$$\frac{St_{PK}/St_{FP}}{(P_2/P_1)^{0.8}} = \frac{n_{St}\,(M_\infty \text{ Sin } \theta - 1) + 0.75}{\left(\frac{7(M_\infty \text{ Sin } \theta)^2 - 1}{6}\right)^{0.8}} \tag{9}$$

Equation 9 is plotted in Figure 31 and shows the trend in the amplification factor with X/δ.

The location of the peak pressure has been compared to the location of peak heating in Figure 32 to see if they are coincident. For $X/\delta > 10$ the peak locations can be taken as coincident, however in the region at small X/δ the peak heating occurs slightly outboard of the peak pressure location.

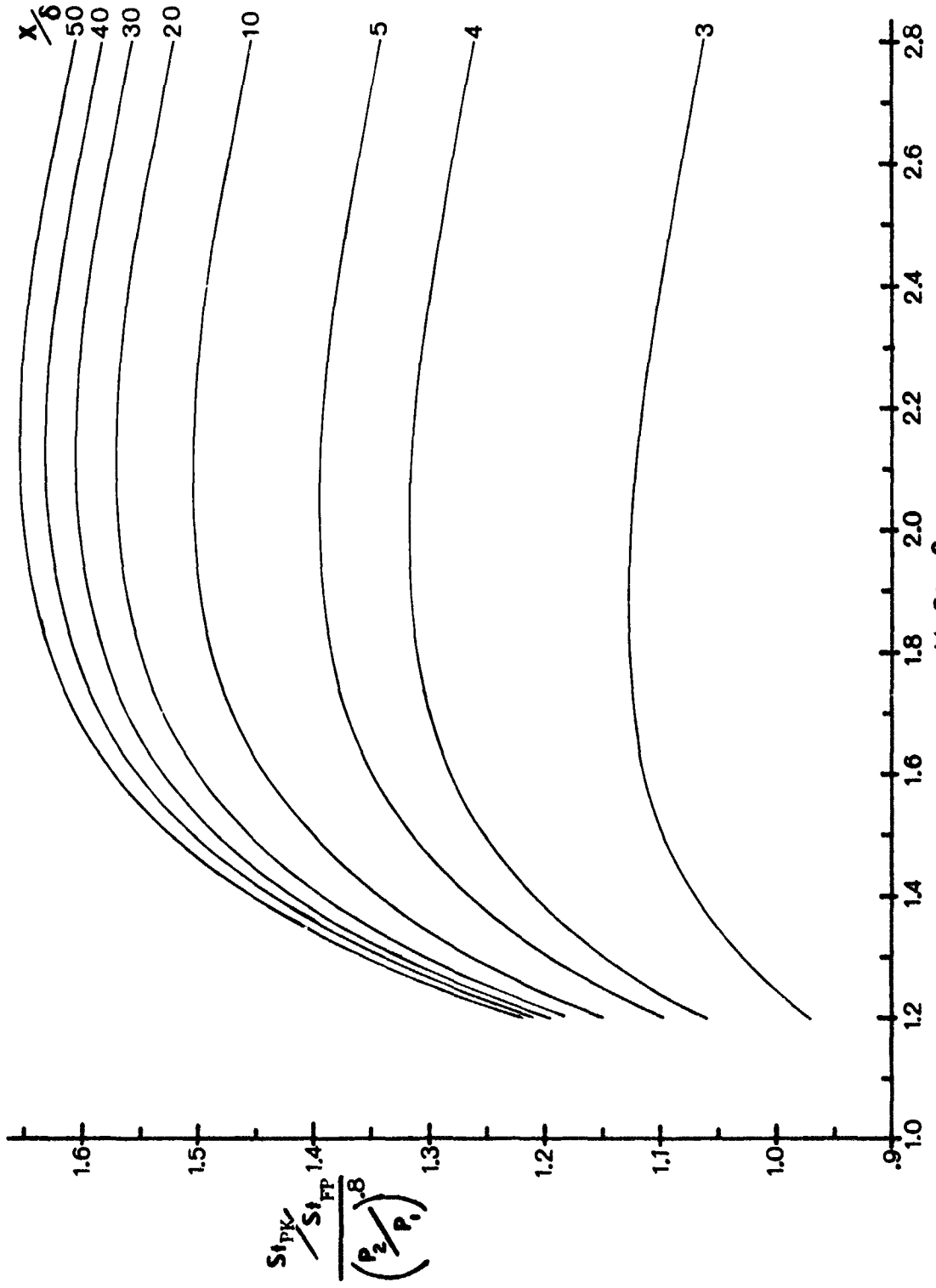

Figure 31. Amplification of Peak Heating Due to Vorticity

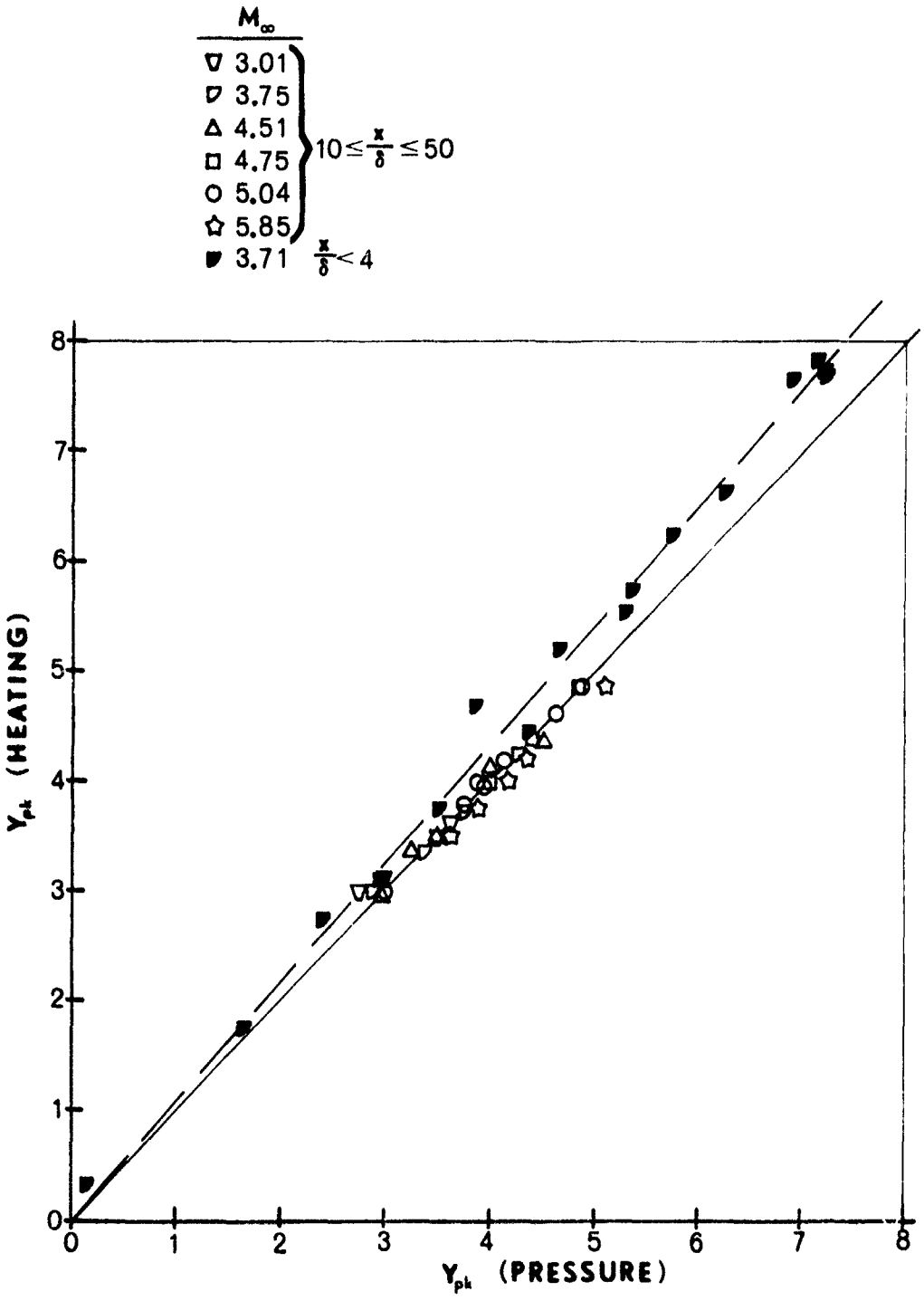

Figure 32. Comparison of Peak Pressure and Heating Location

2. HEAT TRANSFER DISTRIBUTIONS

Token (Reference 2) derived equations based upon stagnation point flow which govern the heat transfer distribution between the peak and the shock locations. The result of his analysis was

$$\frac{h - h_{SH}}{h_{PK} - h_{SH}} = 1 - \left[1 - \frac{\psi}{\psi_{PK}}\right]^{\frac{4n-3}{5}} \left(1 + C\frac{\psi}{\psi_{PK}}\right)^{0.8} \tag{10}$$

where ψ is the independent coordinate measured from the shock wave toward the fin in a direction normal to the fin. "C" is a pressure gradient parameter defined by

$$0 = (P_{PK} - P_{SH})/P_{SH} \tag{11}$$

and "n" is a velocity gradient parameter. In his derivation Token assumed a variation of the velocity gradient with ψ of the form

$$\beta = K\,\psi^{n} \text{ (K constant)} \tag{12}$$

The exponent in Equation 12 is the velocity gradient parameter in Equation 10.

Through the correlation of his data Token observed values for these parameters of

$$n = 0.5; \quad 0.2 \leq C \leq 1$$

where the weighted average for C was 0.41. Using these values Token successfully correlated his data taken at Mach 3.71 and Re = 3.5×10^6 per foot. These values however are not sufficient for the general correlation of the data presented in this report. For large values of the shock strength the pressure gradient parameter is a strong function of "X/δ" and "M_∞ Sin θ" as shown in Figure 33. In this figure the pressure gradient parameter was calculated from the data base and plotted as a function of M_∞ Sin θ . At a fixed shock strength the magnitude of "C" was observed to increase with X/δ but the precise function with

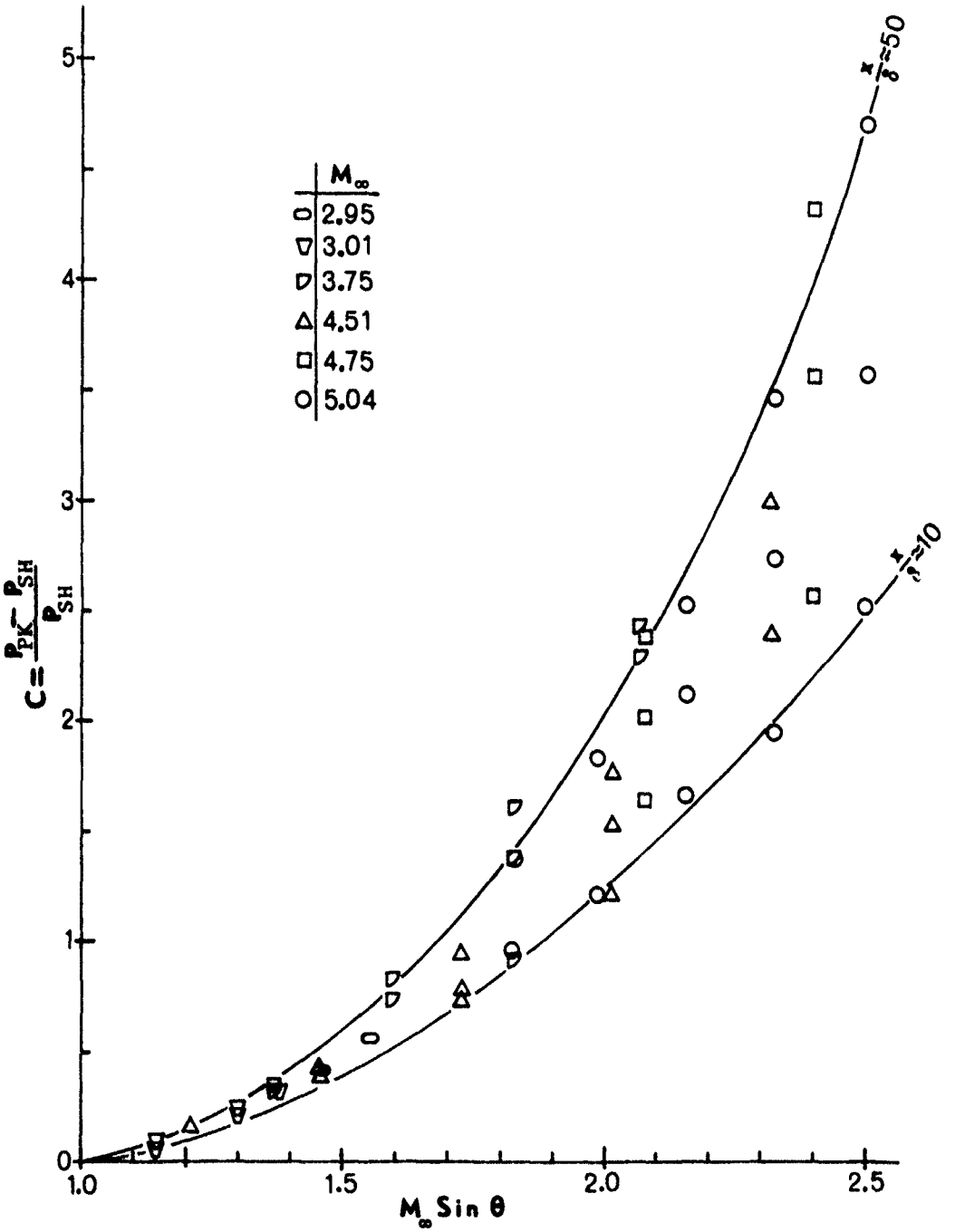

Figure 33. Pressure Gradient Parameter

X/δ could not be defined. The upper and lower curves on Figure 33 approximate the maximum and minimum functions with X/δ covered by the data.

Figure 34 demonstrates the effect of C on Equation 10. It shows that the large values of C predicted by Figure 33 produce unrealistic heating rates for n = 0.5. The value of the velocity gradient must then have a variation range similar to that of the pressure gradient. The value of n for any particular interaction must be found by trial and error as shown in Figure 35. The heating distribution is plotted according to the parameters of Equation 10, the value of C is estimated from Figure 33, and values of n were tried in Equation 10 until a reasonable fit was obtained. Figure 35 shows that n may be as large as 1.75.

Equation 10 may be used to correlate the heating distributions, however to be used as a prediction tool the shock heating rate must be known. Correlation of the heating rate at the shock location was successful only for $M \sin_\infty \theta < 1.7$ as shown in Figure 36. Above $M_\infty \sin \theta = 1.7$ the data trends diverge in a manner which could not be accounted for with the existing data base.

$$c = \frac{P_{PK} - P_{SH}}{P_{SH}}$$

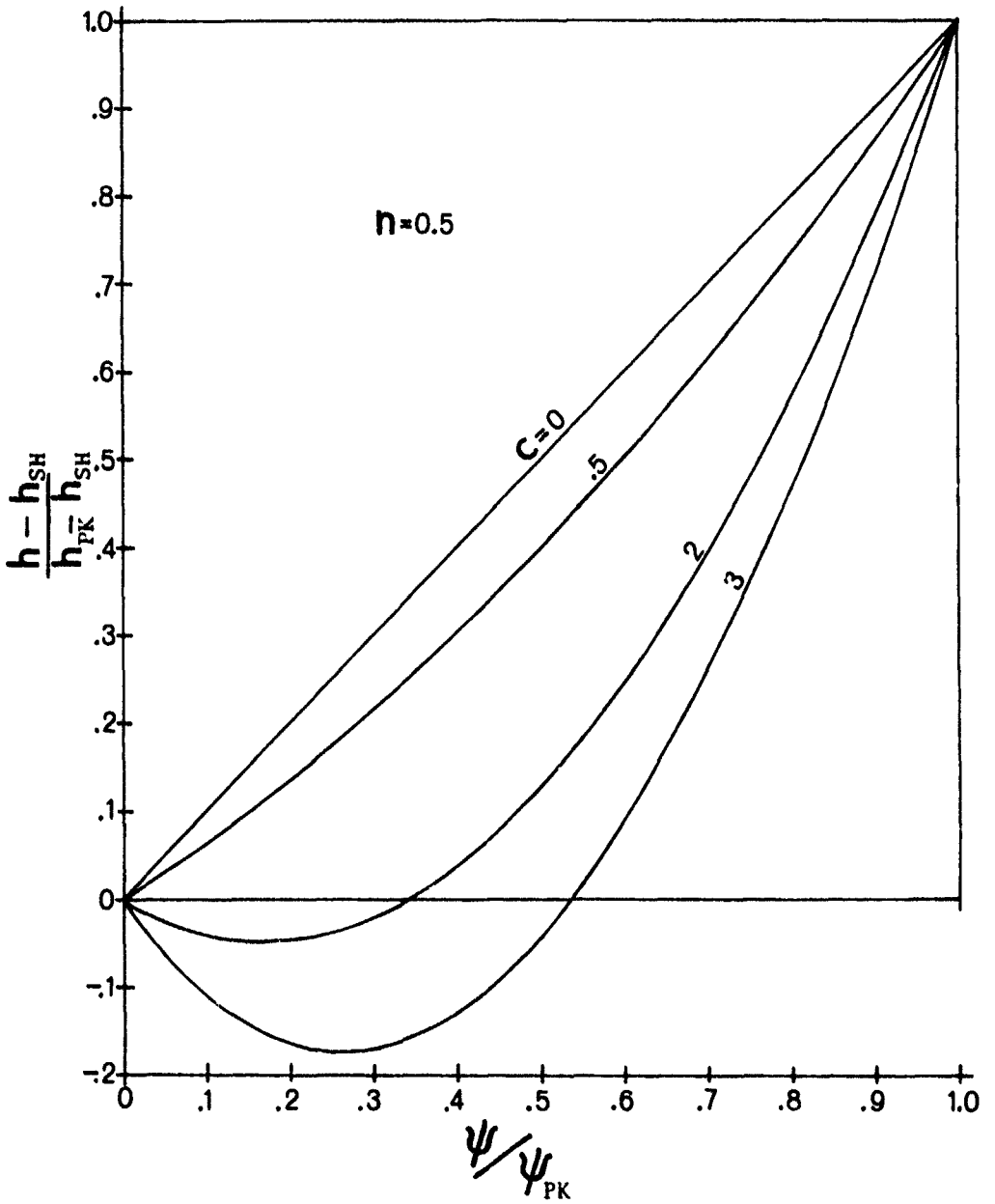

Figure 34. Effect of Pressure Gradient Parameter

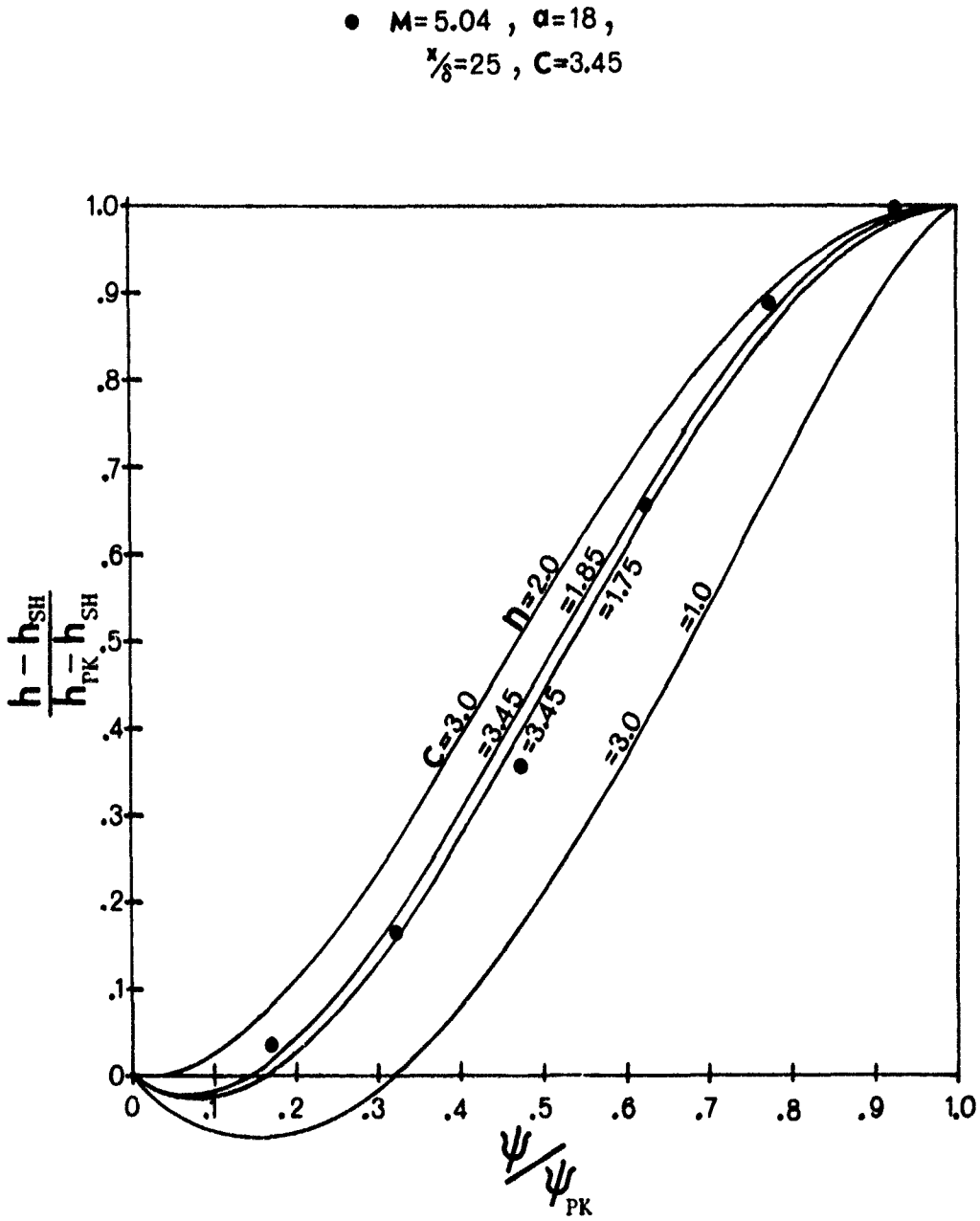

Figure 35. Effect of Velocity Gradient Parameter

	M_∞	x/δ filled	open	flagged	ref
▽	3.01	48	34	19	4
▽	3.75	40	28	15	4
△	4.51	43	30	17	4
□	4.75	25	17	10	5
○	5.04	25	17	10	5

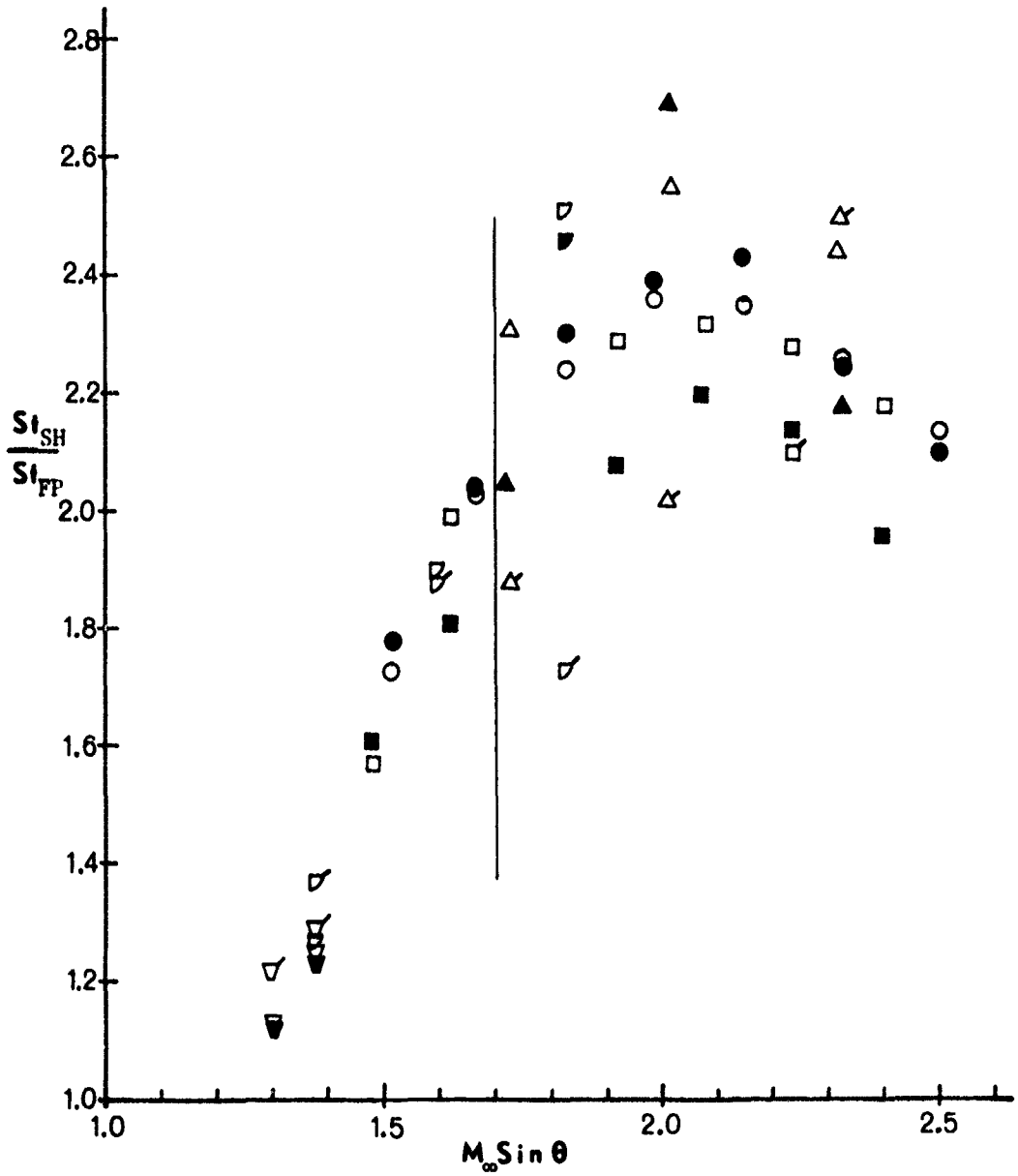

Figure 36. Heating Rate Under the Shock

SECTION IV

CONCLUSIONS

(1) It has been shown that the peak pressure in a 3-D interaction can be predicted by

$$\frac{P_{PK}}{P_{FP}} = (M_\infty \text{ Sin } \theta)^{n_p} \qquad (1)$$

where n_p is a function of X/δ and has a value of 2.4 at large X/δ. Since $n_p = 2.14$ for oblique shock calculations the 3-D interaction can produce peak pressure greater than oblique shock predictions.

(2) Once separation has been established a plateau region develops within the pressure profile which is similar to that in the 2-D interaction. 2-D and 3-D plateau pressure correlate well and separation occurs at 73% of the plateau pressure rise. The location of separation can be predicted by a set of hyperbolic curves defined by Figures 9 to 12.

(3) The peak heating rates in the 3-D interaction are predicted by

$$\frac{St_{PK}}{St_{FP}} = n_{St} (M_\infty \text{ Sin } \theta - 1) + 0.75$$

where n_{St} is a function of X/δ. At large X/δ the value of n_{St} is about 4.75. Since 2-D correlations provide an n_{St} of 2.65 it can be seen that the 3-D interaction produces heating rates which are much more severe than those of a corresponding 2-D interaction.

REFERENCES

1. B. Oskam, S. M. Bogdonoff, I. E. Vas, Study of Three-Dimensional Flow Fields Generated by the Interaction of a Skewed Shock Wave with a Turbulent Boundary Layer, AFFDL-TR-75-21, Air Force Flight Dynamics Laboratory, WPAFB, Ohio. February 1975.

2. K. H. Token, Heat Transfer Due to Shock Wave Turbulent Boundary Layer Interactions on High Speed Weapon System, AFFDL-TR-74-77, Air Force Flight Dynamics Laboratory, WPAFB, Ohio. April 1974.

3. Unpublished data taken at Mach 3.0 and 3.71, Reynolds number per foot of 3.5 x 10^6 in the NASA Langley UPWT. Boundary layer thickness at the fin leading edge ranged from 0.37 to 0.43 inches.

4. R. D. Neumann, K. H. Token, "Prediction of Surface Phenomena Induced by Three-Dimensional Interactions on Planar Turbulent Boundary Layers", International Astronautical Federation XXVth Congress, Paper No. 74-058, 30 September - 5 October 1974.

5. R. D. Neumann, J. R. Hayes, "Prediction Techniques for the Characteristics of Three-Dimensional Shock Wave/Turbulent Boundary Layer Interactions", AIAA 15th Aerospace Sciences Meeting, Paper No. 77-46, 24-26 January 1977.

6. R. G. Christophel, W. A. Rockwell, Tabulated Mach 6 3-D Shock Wave Turbulent Boundary Layer Interaction Heat Transfer Data, AFFDL-TM-74-212-FXG, Air Force Flight Dynamics Laboratory, WPAFB, Ohio. November 1974.

7. S. M. Bogdonoff, "Some Experimental Studies of the Separation of Supersonic Turbulent Boundary Layers", Princeton Univ. Aeronautical Eng'g Dept. Report 336, Princeton, New Jersey, June 1975.

8. F. W. Spaid, "Two-Dimensional Jet Interaction Studies at Large Value of Reynolds and Mach Numbers", AIAA-J Vol. 13, No. 11, November 1975, pp. 1430-1434.

9. R. Wilson, F. Maurer, An Experimental Investigation of Turbulent Separated Boundary Layers at Low Supersonic Mach Numbers" Deutsche Luft- and Raumfahrt, DLR FB 70-33, August 1970.

10. E. E. Zukoski, "Turbulent Boundary Layer Separation in Front of a Forward Facing Step", AIAA-J Vol. 5, No. 10, October 1967, pp. 1746-1753.

11. V. S. Dem'yanko, V. A. Igumnov, "Spatial Shock Wave-Turbulent Boundary Layer Interactions in the Interference Region of Intersecting Surfaces", Izvestiya Sibirskogo Otdeleniya Akademii Nauk SSSR, Seriya Tekhnicheskikh Nauk, Izd-vo "Nauka", Novosibirsk, Nr. 8(248), Issue 2 June 1975, pp 56-62.

REFERENCES (Cont'd)

12. V. S. Avduevskii, V. K. Gretsov, "Investigation of the Three-Dimensional Separation Flow Around Half Cones on a Flat Plate", Izvestiya Akademii Nauk SSSR, Mekhanika ZhidKosti i Gaza, No. 6 pp. 112-115, Nov-Dec 1970.

13. R. H. Korkegi, "Simple Correlation for Incipient Turbulent Boundary Layer Separation Due to Skewed Shock Wave", AIAA-J, Vol. 2, No. 2, November 1973, pp. 1578-1579.

14. B. Oskam, S. M. Bogdonoff, I. E. Vas, Oblique Shock Wave/Turbulent Boundary Layer Interactions in Three-Dimensions at Mach 3, AFFDL-TR-76-48, Air Force Flight Dynamics Laboratory, WPAFB, Ohio, June 1976.

15. R. D. Neumann, G. L. Burke, The Influence of Shock Wave-Boundary Layer Effects on the Design of Hypersonic Aircraft, AFFDL-TR-68-152, Air Force Flight Dynamics Laboratory, WPAFB, Ohio, March 1959.

☆ U S GOVERNMENT PRINTING OFFICE: 1977 — 757-001/529